

This is the accepted manuscript made available via CHORUS. The article has been published as:

Signatures of extra dimensions in gravitational waves from black hole quasinormal modes

Sumanta Chakraborty, Kabir Chakravarti, Sukanta Bose, and Soumitra SenGupta

Phys. Rev. D **97**, 104053 — Published 29 May 2018

DOI: [10.1103/PhysRevD.97.104053](https://doi.org/10.1103/PhysRevD.97.104053)

Signatures of extra dimensions in gravitational waves from black hole quasi-normal modes

Sumanta Chakraborty,^{1,*} Kabir Chakravarti,^{2,†} Sukanta Bose,^{2,3,‡} and Soumitra SenGupta^{1,§}

¹*Theoretical Physics Department, Indian Association for the Cultivation of Science, Kolkata 700032, India*

²*IUCAA, Ganeshkhind, Post Bag 4, Pune University Campus, Pune 411007, India*

³*Department of Physics & Astronomy, Washington State University,
1245 Webster, Pullman, WA 99164-2814, U.S.A*

In this work we have derived the evolution equation for gravitational perturbation in four dimensional spacetime in presence of a spatial extra dimension. The evolution equation is derived by perturbing the *effective* gravitational field equations on the four dimensional spacetime, which inherits non-trivial higher dimensional effects. Note that this is *different* from the perturbation of the five dimensional gravitational field equations, existing in literature, and possesses quantitatively new features. The gravitational perturbation has further been decomposed into a purely four dimensional part and another piece that depends on extra dimensions. The four dimensional gravitational perturbation now admits massive propagating degrees of freedom, owing to the existence of higher dimensions. We have also studied the influence of these massive propagating modes on the quasi-normal mode frequencies, signaling the higher dimensional nature of the spacetime, and have contrasted these massive modes with the massless modes in general relativity. Surprisingly, it turns out that the massive modes experience much smaller damping compared to the massless modes in general relativity and may even *dominate* over and above the general relativity contribution if one observes the ringdown phase of a black hole merger event at sufficiently late times. Furthermore, the whole analytical framework has been supplemented by the fully numerical Cauchy evolution problem as well. In this context we have shown that except for minute details the overall features of the gravitational perturbations are captured in both the Cauchy evolution as well as in the analysis of quasi-normal modes. The implications on observations of black holes with LIGO and proposed space missions like LISA are also discussed.

PACS numbers: 04.30.-w, 04.50.+h, 04.50.Gh

Keywords: Higher Dimensions; Gravitational Waves; Quasi-normal Modes; Cauchy Evolution

I. INTRODUCTION

Unification of forces has been the most challenging task the science community has ever faced. So far that quest has successfully brought the electromagnetic, strong and weak forces under one roof. However the unification scheme hits a wall when one tries to incorporate in it the only other fundamental force, namely, gravity. There have been numerous attempts, so far, to incorporate gravity in the above picture as well, leading to a unified quantum theory of nature. This has resulted in a large number of candidate theories for quantum gravity, *but* without much success. This issue, broadly speaking, originates from the peculiar fact that the energy scale associated with grand unified theories is $\sim \mathcal{O}(10^3)\text{GeV}$, while the natural energy scale for gravity is the Planck scale $\sim \mathcal{O}(10^{18})\text{GeV}$. This huge difference between the respective energy scales manifests itself into unnatural fine tunings in various physical parameters of the model, e.g., in the mass of the Higgs Boson. Thus it seems legitimate to understand the origin of this fine tuning problem (known as the *gauge hierarchy problem*) before delving into quantization of gravity [1–7].

One such natural candidate for resolving the gauge hierarchy problem in this regard corresponds to extra spatial dimensions, which can bring down the Planck scale to the realm of grand unified theories. Such a possibility was considered in [8–12] where the extra dimensions were large enough, such that the volume spanned by them could suppress the Planck scale of the higher dimensional spacetime (known as *bulk*) to the TeV scale. However this proposal harbours two conceptual drawbacks: Firstly, it seems that the problem of energy scale hierarchy has merely been transferred to another form, the volume hierarchy, e.g., if one wants to reduce the energy scale to 1 TeV the size of the extra dimensions would be $\sim 10^{11}$ m; and more importantly it treats the higher dimensional spacetime

*Electronic address: sumantac.physics@gmail.com

†Electronic address: kabir@iucaa.in

‡Electronic address: sukanta@iucaa.in

§Electronic address: tpssg@iacs.res.in

to be flat [1]. The second one is indeed a serious issue, as gravity cannot be shielded and hence if it is present in four dimensions gravity is bound to propagate in higher spacetime dimensions as well. In order to cure this problem, Randall and Sundrum proposed a very natural solution to the hierarchy problem with warped extra dimensions, where presence of gravity in higher dimensions forces the effective Planck scale to reduce to TeV scale in the four dimensional hypersurface we live in (known as *brane*) [13, 14]. This scenario has been extensively studied in the literature in the past years in various contexts, starting from black holes [15–22] and cosmology [23–32] to particle phenomenology as well as possible signatures in Large Hadron Collider (LHC) [33–35]. A lot of attention has also been devoted to the higher curvature generalization of this scenario, obtained by introducing terms like R^2 , $R_{abcd}R^{abcd}$ in the gravitational action, as well as to the stabilization of these extra dimensions [23, 36–40].

Even though LHC provides us an observational window for the existence of extra spatial dimensions, it is important to know if there exists any other observational tests that can either prove or disprove their existence independently. It is obvious that in order to probe these effects, one has to investigate high energy/high curvature regime, which can originate from either high energy collisions like in LHC or from physics near black holes. The second possibility opens up a few interesting observational avenues — (a) the black hole continuum spectrum, originating from accretion disc around a supermassive black hole, (b) strong gravitational lensing around supermassive black holes and finally, (c) gravitational waves from collision of two massive black holes. We have already elaborated on the continuum spectrum from supermassive black holes and their implications regarding the presence of extra dimensions in [41], while strong gravitational lensing has been discussed in detail in [42]. In this work we aim to address the third possibility, i.e., the effect of higher dimensions on gravitational waves, in light of the recent detections [43–47] of the same in Advanced Laser Interferometer Gravitational-Wave Observatory (aLIGO). The whole process of collision between two black holes can broadly be divided into three categories — inspiral phase, merger phase and ringdown phase. The first two phases are best described by a combination of post-Newtonian and numerical approaches [48–63], which we leave for the future, concentrating here on the ringdown phase only. In this situation the quasi-normal mode frequencies play a very fundamental role in determining the ring down phase and in this work we will concentrate on deriving the quasi-normal mode frequencies for this higher dimensional scenario [16, 19, 64–67].

To understand the behaviour of quasi-normal mode frequencies in the context of higher spacetime dimensions, one can follow two possible approaches — (a) One starts from the gravitational field equations in the bulk and then consider its perturbation around a bulk solution, which manifests itself as a black hole on the brane. This one we refer to as the *bulk based approach*. (b) Otherwise, one projects the bulk gravitational field equations on the brane hypersurface resulting in an effective description of the brane dynamics inherited from the bulk, referred to as the *brane based approach*. In this case as well one perturbs the effective gravitational field equations on the brane, around a given bulk solution representing again a brane black hole. Some aspects of this problem along the first line of attack has already been elaborated and explored in [68–74], while to our knowledge the second avenue is hitherto unexplored. In this work, we wish to fill this gap by providing a thorough analysis of the second approach in relation to the black hole perturbation theory and possible discords with the bulk based approach. In particular, we will try to understand whether the results derived in [68] using Cauchy evolution of initial data matches with our quasi-normal mode frequency analysis. Further for completeness we will present the Cauchy evolution for the brane based approach as well. This will not only help to contrast these two approaches but will also depict whether the quasi-normal mode analysis and the Cauchy evolution are compatible with each other. Besides providing yet another independent route towards understandings of higher dimensions, this will also be of significant interest to the gravitational wave community.

The paper is organized as follows: We start in Section II with a brief introduction of the effective equation formalism in the context of higher spatial dimensions and then we build up our gravitational perturbation equation based on the above. This has been applied in Section III to derive the evolution equations for the master variables associated with spherically symmetric brane and possible effects from higher dimensions. In Section IV we have studied these perturbation equations in Fourier space and have derived the quasi-normal mode frequencies using the continued fraction method as well as the direct integration scheme. Using these quasi-normal mode frequencies the time evolution of the master variable has been determined for both the bulk and the brane based approach in Section V. Section VI deals with Cauchy evolution of the initial data and its possible harmony with the quasi-normal mode analysis. We conclude with a discussion and implications of the results obtained, in Section VII. Some detailed calculations pertaining to derivation of gravitational perturbation equation on the brane have been presented in Appendix A, while those associated with continued fraction method have been elaborated in Appendix B.

Notations and Conventions: We will set the fundamental constant c as well as the combination GM to unity, where M is the mass of the black hole. Indices running over all the bulk coordinates are denoted by uppercase Latin letters, while all the brane indices are denoted by Greek letters. Any geometrical quantity associated with the brane hypersurface alone is being denoted with a superscript (4). Further, all the matrix valued quantities will be denoted by boldfaced letters. Finally the signature convention adopted in this work is the mostly positive one.

II. PERTURBING EFFECTIVE GRAVITATIONAL FIELD EQUATIONS ON THE BRANE

We start this section by providing a very brief introduction to the effective gravitational field equations on the brane, which will be necessary for our later purposes. Since we are interested in signatures of higher dimensions only, it will be sufficient to work within the context of Einstein gravity in five spacetime dimensions, in which case the gravitational Lagrangian density is the five dimensional Ricci scalar R . Thus the five dimensional gravitational field equations will read $G_{AB} = 8\pi G_{(5)} T_{AB}$, where T_{AB} stands for the matter energy momentum tensor, which may be present in the bulk and $G_{(5)}$ is the five dimensional gravitational constant. In the specific context when the bulk energy momentum tensor is originating from a negative cosmological constant Λ , one arrives at the following static and spherically symmetric solution on the brane,

$$ds_{\text{unperturbed}}^2 = e^{-2ky} \left(-f(r)dt^2 + \frac{dr^2}{f(r)} + r^2 d\Omega^2 \right) + dy^2, \quad (1)$$

with $f(r) = 1 - (2/r)$ and $k \propto \sqrt{-\Lambda}$. Note that from the perspective of a brane observer located on a $y = \text{constant}$ hypersurface, the spacetime structure on the brane is given by the Schwarzschild solution.

This raises the following interesting question: What happens to the gravitational field equations on the brane, given the gravitational field equations on the bulk? It has been answered for Einstein gravity in [75] and has been extended recently to various other scenarios involving alternative gravity theories [76–78]. The derivation goes as follows, one first chooses the brane hypersurface, say $y = 0$, and determines the normal $n_A = \nabla_A y$, yielding the induced metric on the brane hypersurface to be $h_{AB} = g_{AB} - n_A n_B$, such that $n_A h_B^A = 0$. Given the induced metric, one can introduce the notion of covariant derivative on a brane hypersurface and hence a notion of brane curvature using commutator between the brane covariant derivatives. This enables one to express the bulk curvature in terms of the brane curvature and extrinsic curvatures associated with the brane hypersurface. Further contractions will enable one to relate the bulk Einstein's equations with curvatures on the brane, referred to as the effective gravitational field equations on the brane. The effective equations in vacuum brane differ from four dimensional Einstein's equations by an additional term inherited from the bulk Weyl tensor and takes the following form,

$$^{(4)}G_{\mu\nu} + E_{\mu\nu} = 0. \quad (2)$$

Here $E_{\mu\nu}$ stands for a particular projection of the bulk Weyl tensor C_{ABCD} on the brane hypersurface (commonly known as the electric part) given by,

$$E_{\mu\nu} = C_{ABCD} e_\mu^A n^B e_\nu^C n^D, \quad (3)$$

where n_A is the normalized normal introduced earlier and $e_\mu^A = \partial x^A / \partial y^\mu$ is the bulk to brane projector, with x^A being the bulk coordinates and y^μ are the brane coordinates [79, 80].

At this stage it is worth mentioning that in order to arrive at the above relation we have assumed that the bulk cosmological constant and the brane tension cancels each other, leading to a vanishing effective cosmological constant on the brane hypersurface [13, 75]. The above cancellation has its origin in the fact that in the effective field equation the effective cosmological constant is the difference between bulk cosmological constant and brane tension, and this difference has to be zero for the stability of the background spacetime. Further, note that even though Eq. (2) acts as the effective field equations on the brane, to solve it explicitly one does require information of the bulk, hidden in $E_{\mu\nu}$ through the bulk Weyl tensor.

There are two ways to solve this equation — (a) Assume certain bulk geometry as ansatz (which for our case corresponds to Eq. (1)) and then try to see what sort of brane configuration solves Eq. (2). (b) Take $E_{\mu\nu}$ as an arbitrary tensor and try to solve Eq. (2) with $E_{\mu\nu}$ treated as a source: e.g., in the context of spherical symmetry one often divides $E_{\mu\nu}$ into an energy density (known as *dark radiation*) and pressure (known as *dark pressure*). Even though one can have very interesting results emerging from the second scenario [81], it has the drawback that the bulk metric remains unknown and in general it is not even clear whether there exists a bulk metric that would satisfy Einstein's equations in the bulk. Thus we will adopt the first scenario and shall take Eq. (1) as the background metric which indeed satisfies Eq. (2) as well [76, 81–84].

This procedure must be contrasted with the perturbation of bulk Einstein's equations around the solution presented in Eq. (1), since in the case of effective field equations, the perturbation of bulk Weyl tensor will play a crucial role. Thus it is not at all clear a priori how the perturbed equations in the brane based approach will behave in contrast to the bulk based approach, even though they are being perturbed around the same solution. With this motivation in the backdrop, let us concentrate on perturbation of Eq. (3) around the bulk metric g_{AB} given in Eq. (1), such that,

$$g_{AB} \rightarrow g_{AB} + h_{AB}. \quad (4)$$

Here h_{AB} is the perturbed metric around g_{AB} and all the expressions to follow will be evaluated to the first order in the perturbed metric h_{AB} ¹.

It is also well known that not all the components of h_{AB} are dynamical, there are redundant gauge degrees of freedom. These gauge choices must be made according to convenience of calculations. In this particular situation the following gauge conditions will turn out to be useful later on,

$$\nabla_A h_B^A = 0; \quad h_A^A = 0; \quad h_{AB} = h_{\alpha\beta} e_A^\alpha e_B^\beta, \quad (5)$$

known as the Randall-Sundrum gauge. The usefulness of this gauge condition can also be anticipated from the fact that these imply $h_{AB} n^A = 0$ and hence the perturbed bulk metric takes the following form,

$$ds_{\text{perturbed}}^2 = \left[q_{\alpha\beta}(y, x^\mu) + h_{\alpha\beta}(y, x^\mu) \right] dx^\alpha dx^\beta + dy^2, \quad (6)$$

where $q_{\alpha\beta}$ solves Eq. (2) and is given by

$$\begin{aligned} q_{\alpha\beta} dx^\alpha dx^\beta \\ = e^{-2ky} \left(-f(r) dt^2 + \frac{dr^2}{f(r)} + r^2 d\theta^2 + r^2 \sin^2 \theta d\phi^2 \right). \end{aligned} \quad (7)$$

Even though Eq. (1) opts for $f(r) = 1 - (2/r)$, in the rest of the analysis we will keep $f(r)$ as general as possible. Then to linear order in the perturbed metric $h_{\alpha\beta}$ one can expand the four dimensional Einstein tensor as,

$$\begin{aligned} {}^{(4)}G_{\mu\nu} \simeq {}^{(4)}G_{\mu\nu}^{(q)} + {}^{(4)}R_{\mu\nu}^{(h)} \\ - \frac{1}{2} q_{\mu\nu} {}^{(4)}R^{(h)} - \frac{1}{2} h_{\mu\nu} {}^{(4)}R^{(q)}, \end{aligned} \quad (8)$$

where terms with superscript (q) denote that they have to be evaluated for the brane background metric $q_{\alpha\beta}$ given in Eq. (7) and superscript (h) implies that it has been evaluated for the perturbed metric $h_{\mu\nu}$. The index (4) implies that these are all four dimensional geometrical quantities.

Another ingredient in the perturbation of effective brane based approach is the perturbation of the bulk Weyl tensor. For that one has to write down the bulk Weyl tensor in terms of the bulk Riemann, Ricci tensor and Ricci scalar and expand all of them to leading order in the gravitational perturbation $h_{\alpha\beta}$. The above procedure leads to,

$$\begin{aligned} C_{ABCD} &= R_{ABCD} - \frac{1}{3} R_{AC} g_{BD} + \frac{1}{3} R_{AD} g_{BC} + \frac{1}{3} R_{BC} g_{AD} - \frac{1}{3} R_{BD} g_{AC} + \frac{1}{12} R (g_{AC} g_{BD} - g_{AD} g_{BC}) \\ &\simeq C_{ABCD}^{(g)} + \left\{ R_{ABCD}^{(h)} - \frac{1}{3} R_{AC}^{(g)} h_{BD} - \frac{1}{3} R_{AC}^{(h)} g_{BD} + \frac{1}{3} R_{AD}^{(h)} g_{BC} + \frac{1}{3} R_{AD}^{(g)} h_{BC} - \frac{1}{3} R_{BD}^{(h)} g_{AC} \right. \\ &\quad - \frac{1}{3} R_{BD}^{(g)} h_{AC} + \frac{1}{3} R_{BC}^{(h)} g_{AD} + \frac{1}{3} R_{BC}^{(g)} h_{AD} + \frac{1}{12} R^{(h)} (g_{AC} g_{BD} - g_{AD} g_{BC}) \\ &\quad \left. + \frac{1}{12} R^{(g)} (g_{AC} h_{BD} + h_{AC} g_{BD} - g_{AD} h_{BC} - h_{AD} g_{BC}) \right\}. \end{aligned} \quad (9)$$

Here superscript (g) denotes that the respective quantity is evaluated for the bulk background metric g_{AB} . Note that due to dependence of $q_{\alpha\beta}$ on extra dimensional coordinate y , quantities evaluated for the bulk metric will inherit y -derivatives of $q_{\alpha\beta}$ and hence will differ from their four-dimensional counterparts. Given the perturbation of bulk Weyl tensor the corresponding projection of the perturbed bulk Weyl tensor onto the brane hypersurface results in,

$$\begin{aligned} E_{\mu\nu} \simeq E_{\mu\nu}^{(g)} + \left\{ R_{ABCD}^{(h)} e_\mu^A n^B e_\nu^C n^D - \frac{1}{3} R_{AC}^{(h)} e_\mu^A e_\nu^C \right. \\ \left. - \frac{1}{3} R_{BD}^{(h)} n^B n^D q_{\mu\nu} - \frac{1}{3} R_{BD}^{(g)} n^B n^D h_{\mu\nu} + \frac{1}{12} R^{(h)} q_{\mu\nu} + \frac{1}{12} R^{(g)} h_{\mu\nu} \right\}. \end{aligned} \quad (10)$$

¹ In principle one should write down $g_{AB} \rightarrow g_{AB} + \epsilon h_{AB}$, with small ϵ and then keeping only terms linear in ϵ .

Note that in the above perturbation equation for the projected bulk Weyl tensor, the first order corrections to bulk Riemann, Ricci tensor and Ricci scalar appears. One can decompose all these perturbed quantities evaluated for the bulk metric in terms of the respective brane metric and extra dimensional contributions. This has been explicitly carried out in [Appendix A](#) and ultimately leads to the following expression for the projected bulk Weyl tensor,

$$\begin{aligned} E_{\mu\nu}^{(h)} = & \frac{1}{6} {}^{(4)}\square h_{\mu\nu} - \frac{1}{3} \partial_y^2 h_{\mu\nu} - k \partial_y h_{\mu\nu} + \frac{1}{3} k^2 h_{\mu\nu} \\ & + \frac{1}{3} h_\beta^\alpha {}^{(4)}R_{\mu\alpha\nu}^{(q)\beta} - \frac{1}{6} h_\mu^\alpha {}^{(4)}R_{\alpha\nu}^{(q)} \\ & - \frac{1}{6} h_\nu^\alpha {}^{(4)}R_{\alpha\mu}^{(q)} + \frac{1}{12} {}^{(4)}R^{(q)} h_{\mu\nu} . \end{aligned} \quad (11)$$

At this stage it is worth emphasizing that the gauge conditions elaborated in [Eq. \(5\)](#), take a simpler form in this context. In particular, the spatial part of the differential condition $\nabla_A h_\mu^A = 0$, when expanded in terms of four dimensional quantities immediately yields $\nabla_\nu h_\mu^\nu = 0$. Use of this relation and commutator of four dimensional covariant derivative results into $\nabla^\mu E_{\mu\nu}^{(h)} = 0$, as is evident from [Eq. \(11\)](#) in the context of vacuum solutions.

One can also try to understand this result from a different perspective. Since we are perturbing around vacuum solutions, it follows from [Eq. \(2\)](#) that $E_{\mu\nu}^{(h)} \propto {}^{(4)}G_{\mu\nu}^{(h)}$. Thus it immediately implies that $\nabla_\mu E^{(h)}{}^{\mu\nu} = 0$ as it should be, by virtue of Bianchi identity. Finally collecting all the pieces from perturbation of bulk Weyl tensor elaborated in [Eq. \(11\)](#) as well as perturbation of original Einstein tensor as in [Eq. \(8\)](#) we obtain,

$$\begin{aligned} e^{2ky} \left\{ {}^{(4)}\square h_{\mu\nu} + 2h_{\alpha\beta} {}^{(4)}R_{\mu}{}^{\alpha}{}_{\nu}{}^{\beta} \right\} \\ + \left\{ -k^2 h_{\mu\nu} + 3k \partial_y h_{\mu\nu} + \partial_y^2 h_{\mu\nu} \right\} = 0 . \end{aligned} \quad (12)$$

In order to arrive at the above relation we have used the fact that $q_{\alpha\beta} = \exp(-2ky)g_{\alpha\beta}$, where in this particular situation $g_{\alpha\beta}$ is the Schwarzschild metric. Note that we have not used this fact explicitly anywhere in this section, except for assuming that $g_{\alpha\beta}$ must satisfy vacuum Einstein's equations on the brane. Further, all the geometrical quantities present in the above equation are evaluated for the brane metric $g_{\alpha\beta}$.

At this stage it is instructive to split the perturbation equations into parts depending on four dimensional spacetime and those depending on extra dimensions, such that, $h_{\alpha\beta}(y, x^\mu) = h_{\alpha\beta}(x^\mu)\chi(y)$. Following the separability of the perturbed metric, the above equations can also be decomposed into two parts, which for vacuum brane solution reduce to,

$$e^{-2ky} \left\{ -k^2 \chi + 3k \partial_y \chi + \partial_y^2 \chi \right\} = -\mathcal{M}^2 \chi(y) , \quad (13)$$

$${}^{(4)}\square h_{\mu\nu} + 2h_{\alpha\beta} {}^{(4)}R_{\mu}{}^{\alpha}{}_{\nu}{}^{\beta} - \mathcal{M}^2 h_{\mu\nu} = 0 . \quad (14)$$

Remarkably, the effect of the whole analysis is just the emergence of a massive gravitational perturbation modes. With $\mathcal{M} = 0$, one immediately recovers the dynamical equation governing gravitational perturbation in a non-trivial background. As we will see later, [Eq. \(13\)](#) will lead to a series of masses denoted by m_n and is called the n th Kaluza-Klein mode mass of gravitational perturbation. For each Kaluza-Klein mode, say of order n , there will be a solution $h_{\mu\nu}^{(n)}$ to [Eq. \(14\)](#). When all these n values are summed over one ends up with the full solution of the gravitational perturbation.

To summarize, we have started from the effective gravitational field equations on the 3-brane, which depends on the bulk Weyl tensor and hence on the bulk geometry. The main problem of this approach being, not all the components of the projected bulk Weyl tensor $E_{\mu\nu}$ are determined in terms of quantities defined on the brane. In particular, the transverse-traceless part of the projected bulk Weyl tensor, representing the graviton modes in the bulk spacetime, can not be determined. This is intimately related to the fact that the effective field equations on the brane are *not* closed [\[75\]](#). In this work, we have circumvented this problem by using the gauge freedom for the gravitational perturbation. We have started with the Schwarzschild anti-de Sitter spacetime (as in [Eq. \(1\)](#)) which identically satisfies the effective gravitational field equations on the brane. We then consider perturbation around this background, which certainly involves graviton modes propagating in the bulk spacetime. However the use of Randall-Sundrum gauge (presented in [Eq. \(5\)](#)) enables one to reduce the number of propagating degrees of freedom and hence the effective field equations (at least in the perturbative regime) becomes closed. Finally the method of separation of variables enables one to separate a four dimensional part from the extra dimensional one and arrives at [Eq. \(13\)](#) and [Eq. \(14\)](#) respectively. The presence of extra dimension essentially translates into the infinite tower of Kaluza-Klein modes as far as the propagation of gravitational wave in four dimension is considered.

Let us now emphasise the key differences between our approach and the bulk based one. Interestingly, [Eq. \(14\)](#) governing the evolution of gravitational perturbation of the four dimensional brane is identical to that of bulk based

approach, while the eigenvalue equation, i.e., Eq. (13) determining the mass of graviton is different. Hence the Kaluza-Klein mass modes of graviton in the brane based approach will be different from that in the bulk based approach and hence will have interesting observational consequences in both high energy collision experiments as well as in propagation of gravitational waves. In this work we will mainly be interested in the effect of the mass term originating from Eq. (14), in particular how it modifies the behaviour of perturbations in contrast to general relativity and also how the brane and bulk based approach differs. This is what we will concentrate on in the next sections.

III. SPECIALISING TO SPHERICALLY SYMMETRIC VACUUM BRANE

We have described a general method for deriving the dynamical equations pertaining to gravitational perturbation, starting from the effective gravitational field equations on the brane in the previous section. We would now like to apply the above scenario in the context of black holes on the brane. In particular we are interested in perturbations around the background given by Eq. (1). Thus in this section, with the above scenario in the backdrop, we specialise to vacuum and spherically symmetric solution on the brane, such that, $g_{\alpha\beta} = \text{diag}(-f(r), f^{-1}(r), r^2, r^2 \sin^2 \theta)$. For the moment we concentrate on situations with arbitrary choices for $f(r)$, while later on we will choose a specific form for $f(r)$, namely, $f(r) = 1 - (2/r)$. Further being a vacuum solution, the Ricci tensor and Ricci scalar identically vanishes.

The main focus now will be understanding the evolution equation of the gravitational perturbation $h_{\mu\nu}$ before discussing the Kaluza-Klein modes. In general the perturbation $h_{\mu\nu}$ can depend on all the spacetime coordinates (t, r, θ, ϕ) . The spherical symmetry associated with this problem demands a separation between (t, r) and (θ, ϕ) part, which results into decomposition of the angular part into spherical harmonics. In particular, for the gravitational perturbation we obtain,

$$h_{\alpha\beta}^{(n)} = \sum_{l=0}^{\infty} \sum_{m=-l}^l \sum_{i=1}^{10} h_i^{(nlm)}(t, r) \{Y_{lm}^{(i)}\}_{\alpha\beta}(\theta, \phi), \quad (15)$$

where the perturbation $h_{\alpha\beta}$ have been broken up into ten independent parts, separated into $h_i^{(nlm)}$ depending on (t, r) and the rest depending on the angular coordinates. Further, n stands for the Kaluza-Klein mode index, while l is the angular momentum and m being its z -component. The quantities $\{Y_{lm}\}_{\alpha\beta}$ are the tensorial spherical harmonics in four spacetime dimensions. In order to define these tensor harmonics one should introduce the following normalised basis vectors,

$$\begin{aligned} t^\alpha &= \frac{1}{\sqrt{f(r)}} (\partial_t)^\alpha; & r^\alpha &= \sqrt{f(r)} (\partial_r)^\alpha; \\ \theta^\alpha &= \frac{1}{r} (\partial_\theta)^\alpha; & \phi^\alpha &= \frac{1}{r \sin \theta} (\partial_\phi)^\alpha. \end{aligned} \quad (16)$$

It is clear that they are orthogonal to each other, while the factors in the front ensures that they are normalised as well. Given this structure one can introduce an induced metric on the (θ, ϕ) plane such that, $\mu_{\alpha\beta} = g_{\alpha\beta} + t_\alpha t_\beta - r_\alpha r_\beta$, leading to, $t^\alpha \mu_{\alpha\beta} = 0 = r^\alpha \mu_{\alpha\beta}$. One can also define an antisymmetric tensor $\epsilon_{\alpha\beta} = \theta_\alpha \phi_\beta - \phi_\alpha \theta_\beta$. Given this one can construct ten such irreducible representations, which include $t_\alpha t_\beta Y_{lm}$, $\mu_{\alpha\beta} Y_{lm}$ and so on involving no derivatives of Y_{lm} , as well as terms like $r_{(\alpha} \mu_{\beta)\rho} \nabla^\rho Y_{lm}$, $t_{(\alpha} \mu_{\beta)\rho} \nabla^\rho Y_{lm}$ etc. depending on derivatives of Y_{lm} . Among all these choices, three terms among the ten will depend on the antisymmetric combination $\epsilon_{\alpha\beta}$ and will pick up a term $(-1)^{l+1}$ under parity. These we will refer to as *axial perturbations*. On the other hand, the remaining seven components will inherit an extra factor of $(-1)^l$ under parity transformation and are referred to as *polar perturbations*. Thus the spherical harmonic decomposition of $h_{\alpha\beta}^{(n)}$ in Eq. (15) can be further subdivided into axial and polar parts.

The above decomposition is useful in simplifying the algebra further. It is evident that the operators acting on $h_{\alpha\beta}$ in Eq. (14) are invariant under parity. Thus the solutions to Eq. (14) which are eigenfunctions of parity with different eigenvalues decouple from each other. Hence in the present scenario, the polar and axial perturbations differ from each other in parity eigenvalue and hence evolves independently of one another. Further two axial (or, polar) modes having different l and m values also have different eigenvalues under parity and hence they also decouple. Thus one can solve for the evolution of a given l mode for axial (or, polar) perturbation separately.

Due to complicated nature of the polar perturbations, we content ourselves with the axial perturbations only. The angular part of the axial perturbations contain essentially three terms, two depending on single derivative of Y_{lm} , while the third one depends on double derivatives of Y_{lm} . Thus for $l = 0$ all the axial modes identically vanishes and for $l = 1$, the term involving double derivatives of Y_{lm} does not contribute. Hence in what follows we will concentrate

TABLE I: Numerical estimates of the first ten Kaluza-Klein mass modes correct to second decimal place for two possible choices of the inter-brane separation d and bulk curvature scale ℓ have been presented for brane based approach. First Eq. (25) has been solved for z_n and the result has been presented in the second column. Incidentally, the solution for z_n is insensitive to choices of d/ℓ as far as solutions accurate to second decimal places are considered. To avoid any instability present in the problems the inverse of bulk curvature scale has been chosen such that, the mass of lowest lying Kaluza-Klein mode is greater than or equal to 0.43 in geometrised units.

Kaluza-Klein Modes	z_n	Associated Mass	
		$(d/\ell = 20; 1/\ell = 6 \times 10^7)$	$(d/\ell = 30; 1/\ell = 1.3 \times 10^{12})$
n=1	3.56	0.44	0.43
n=2	6.74	0.83	0.82
n=3	9.88	1.22	1.20
n=4	13.03	1.61	1.58
n=5	16.17	2.00	1.98
n=6	19.32	2.39	2.35
n=7	22.48	2.78	2.73
n=8	25.60	3.17	3.11
n=9	28.75	3.56	3.50
n=10	31.89	3.94	3.88

on the $l \geq 2$ scenario. In this case there are two master variables, which we will denote by $u_{n,l}$ and $v_{n,l}$ respectively and their evolution equations read,

$$\begin{aligned} \mathcal{D}u_{n,l} + f(r) \left\{ m_n^2 + \frac{l(l+1)}{r^2} - \frac{6}{r^3} \right\} u_{n,l} \\ + f(r) \frac{m_n^2}{r^3} v_{n,l} = 0 , \end{aligned} \quad (17)$$

$$\mathcal{D}v_{n,l} + f(r) \left\{ m_n^2 + \frac{l(l+1)}{r^2} \right\} v_{n,l} + 4f(r)u_{n,l} = 0 . \quad (18)$$

Here, \mathcal{D} is the differential operator $\partial_t^2 - \partial_{r_*}^2$, where r_* is the tortoise coordinate defined using $f(r)$ as $dr_* = dr/f(r)$. Note that these two differential equations are coupled to each other and provides a complete set. The massless limit also turns out to be interesting. As far as $u_{n,l}$ is concerned Eq. (17) decouples and the corresponding potential reduces to the well known Regge-Wheeler form. The potential for $v_{n,l}$ resembles to that of an electromagnetic field. Note that an identical form for the equations were derived in [68], however from a different perspective. This is due to the fact explained in Section II, i.e, the evolution of gravitational perturbation equation is identical to [68] modulo the Kaluza-Klein decomposition and hence the mass term.

Having discussed the scenario for gravitational perturbation, let us explore the higher dimensional effects, i.e., determination of the mass term by solving Eq. (13). We will be concerned with the even parity eigenfunctions of Eq. (13), as the derivation of effective field equations assume existence of Z_2 symmetry. Further, Eq. (13) being a second order differential equation will require two boundary conditions to uniquely arrive at the solution. Rather than imposing boundary conditions on $\chi(y)$ we will impose boundary conditions in $\partial_y \chi(y)$. Before engaging with the boundary conditions let us solve Eq. (13), which on introduction of the new variable, $\zeta = e^{ky}$, becomes

$$\zeta^{-2} \left\{ -k^2 \chi + k^2 \zeta^2 \frac{d^2 \chi}{d\zeta^2} + 4k^2 \zeta \frac{d\chi}{d\zeta} \right\} + m^2 \chi = 0 , \quad (19)$$

where the following results have been used,

$$\frac{d\chi}{dy} = k\zeta \frac{d\chi}{d\zeta}; \quad \frac{d^2 \chi}{dy^2} = k^2 \zeta^2 \frac{d^2 \chi}{d\zeta^2} + k^2 \zeta \frac{d\chi}{d\zeta} . \quad (20)$$

One can further transform the above equation to a more manageable form by introducing yet another variable ξ , replacing ζ , such that $m\zeta = \xi$ and the transformed version of Eq. (19) takes the following form,

$$k^2 \xi^2 \frac{d^2 \chi}{d\xi^2} + 4k^2 \xi \frac{d\chi}{d\xi} + (\xi^2 - k^2) \chi = 0 . \quad (21)$$

TABLE II: Numerical estimates of the mass of first ten Kaluza-Klein modes have been presented for the bulk based approach, by solving Eq. (25) for $\nu = 2$. It is clear from Table I that the solution z_n of Eq. (25) is different in the bulk based approach in comparison to the brane based one. Among the two sets of choices for the inter-brane separation d and bulk curvature scale ℓ , one is identical to that of brane based approach, while the other slightly differs. Both these situations clearly depict the differences of the Kaluza-Klein mass modes in the brane and the bulk based approach.

Kaluza-Klein Modes	z_n	Associated Mass	
		$(d/\ell = 20; 1/\ell = 6 \times 10^7)$	$(d/\ell = 30; 1/\ell = 1.2 \times 10^{12})$
n=1	3.83	0.47	0.43
n=2	7.01	0.87	0.79
n=3	10.18	1.26	1.14
n=4	13.33	1.65	1.50
n=5	16.46	2.03	1.85
n=6	19.61	2.42	2.20
n=7	22.76	2.81	2.56
n=8	25.91	3.20	2.91
n=9	29.05	3.59	3.26
n=10	32.19	3.98	3.61

The above equation is essentially Bessel's differential equation and hence it's two independent solutions in terms of modified Bessel functions of first and second kinds are

$$\chi(y) = e^{-\frac{3}{2}ky} \left[C_1 J_\nu \left(\frac{me^{ky}}{k} \right) + C_2 Y_\nu \left(\frac{me^{ky}}{k} \right) \right], \quad (22)$$

with $\nu = \sqrt{13}/2$. The departure from bulk based approach should now be evident from the above analysis. The effect of higher dimensions is through the extra dimensional part of the gravitational perturbation, namely $\chi(y)$. This is certainly a discriminating feature between the bulk and the brane based approach, since the order of the Bessel functions appearing in these two approaches to determine the Kaluza-Klein mode masses are different [68]. Thus it is clear that the mass spectrum of our model will be different when compared to the bulk based approach.

Let us briefly point out the reason behind the difference between Kaluza-Klein mode masses when one follows the brane-based approach, on the one hand, and the bulk-based approach, on the other hand. This is basically due to the difference in the gravitational field equations. For example, when perturbing the bulk gravitational field equations, the Weyl tensor plays no role. By contrast, the perturbation of the Weyl tensor plays a central role in the brane-based approach. Therefore, the basic field equations governing dynamics of gravity in the two approaches differ, but the Schwarzschild AdS spacetime is still a solution of both the field equations. Hence, even though the background solution is the same in both cases, the perturbations follow different dynamics pertaining to the fact that field equations themselves are different. This is why the Kaluza-Klein mode masses are also different. An analogy may be helpful here. For instance, the Schwarzschild solution is a solution of both Einstein gravity as well as $f(R)$ gravity. However, the field equations of both these theories are widely different. Thus, the perturbations about the Schwarzschild background will satisfy different evolution equations in these theories (see, for example [16, 85, 86]), like the scenario we are considering in this work. The fact that the field equations in the bulk and brane based approaches are different is known and is manifested in the fact that there exist solutions to the field equations in the brane-based approach, with no bulk correspondence whatsoever [81, 82, 84, 87, 88]. This explains the difference in the masses of the Kaluza-Klein modes associated with the brane and the bulk based approaches respectively.

To find the unknown coefficients C_1 and C_2 we need to impose boundary conditions and as emphasised earlier these conditions will be on derivatives of $\chi(y)$. To make the analysis at par with possible resolutions of the hierarchy problem, we assume the existence of another brane located at some $y = d$. Incidentally, the distance d need not be constant but varying, known as radion field, whose stabilisation would lead to a non-zero inter-brane separation d [36]. We have also neglected effects of brane bending, if any, by assuming that d is a pure constant. Hence the boundary conditions imposed are given by, $[\partial_y + (\nu + (3/2)k)]\chi = 0$ at $y = 0$ and also on the other brane hypersurface at $y = d$. This leads to the following two algebraic equations satisfied by the two unknown coefficients C_1 and C_2 as

$$C_1 J_{\nu-1}(m/k) + C_2 Y_{\nu-1}(m/k) = 0, \quad (23)$$

$$C_1 J_{\nu-1}(\{m/k\}e^{kd}) + C_2 Y_{\nu-1}(\{m/k\}e^{kd}) = 0. \quad (24)$$

Using the first relation one can determine the ratio C_1/C_2 and hence the solution for $\chi(y)$ gets determined except for

an overall normalisation. On the other hand, substitution of the same in Eq. (24) results into the algebraic equation

$$Y_{\nu-1}(m_n/k)J_{\nu-1}(z_n) - J_{\nu-1}(m_n/k)Y_{\nu-1}(z_n) = 0, \quad (25)$$

where $m_n = \{z_n k\}e^{-kd}$ yields an infinite series of solutions for the mass, where n stands for a particular Kaluza-Klein mode. The masses for the first ten Kaluza-Klein modes have been presented in Table I for two different sets of choices of inter-brane separation d and bulk curvature scale $\ell = 1/k$. This has been achieved by first solving for z_n using Eq. (25) and then obtaining the Kaluza-Klein mass m_n .

To see clearly the difference between brane and bulk based approach, we have presented the masses of the first ten lowest lying Kaluza-Klein modes in the context of bulk based approach as well. This requires solving Eq. (25) for z_n with $\nu = 2$. It is evident from Table II that the solutions for z_n are completely different in the two scenarios. In particular the numerical values of z_n in the brane based approach are lower than the corresponding numerical values in the bulk based approach. This results in lowering of the masses of Kaluza-Klein modes in the brane based approach, as evident from Table I and Table II for the choices $d/\ell = 20$ and $\ell^{-1} = 6 \times 10^7$ in geometrised units. The numerical values are so chosen that they are in agreement with other constraints already present in this framework. For example, $d/\ell \geq 13$ is necessary to arrive at the desired warping required to get around the gauge hierarchy problem, while the table top experiment of Newton's law would demand $1/\ell \geq 10^7(M/M_\odot)$ (or, $\ell \leq 0.1$ mm), where M_\odot is the solar mass [89–91]. This explains the choices of d/ℓ as well as that of $1/\ell$. Numerical estimates of the masses of the Kaluza-Klein modes for two such choices of d/ℓ and $1/\ell$ values have been presented in Table I and Table II respectively. Masses of these Kaluza-Klein modes will be used in the next section for determination of the quasi-normal modes for the brane black hole.

At this stage it is worth mentioning about the Gregory-Laflamme instability, which originates due to instability of the bulk metric under perturbation pertaining to long wavelength modes [20, 92–95]. The fact that there exist another brane at $y = d$ helps to evade the instability by providing a cutoff on the long wavelength modes. The separation d between the two branes as well as the bulk curvature scale $\ell \sim 1/k$ (see Eq. (1)) are also bounded by the fact that we have not seen any influence of the extra dimension on the gravitational interaction in our observable universe. The above instability essentially translates through d and ℓ into the mass of the Kaluza-Klein modes and for $m_n \gtrsim 0.43$ the above instability can be avoided, which is also reflected in both the tables depicting masses of the Kaluza-Klein modes (see also [96]).

Finally, given a particular Kaluza-Klein mode n , one can determine the extra dimensional part of the gravitational perturbation as

$$\chi_n(y) = N_n \left[Y_{\nu-1}(m_n/k)J_\nu(\{m_n/k\}e^{ky}) - J_{\nu-1}(m_n/k)Y_\nu(\{m_n/k\}e^{ky}) \right]. \quad (26)$$

Here N_n is the overall normalisation factor and $\nu = \sqrt{13}/2$ is the order of the Bessel functions. Thus the complete solution to the gravitational perturbation can be written in the following form,

$$\begin{aligned} h_{\alpha\beta}(t, r, \theta, \phi; y) = & \sum_{n=0}^{\infty} N_n \left\{ Y_{\nu-1}(m_n/k)J_\nu(\{m_n/k\}e^{ky}) \right. \\ & \left. - J_{\nu-1}(m_n/k)Y_\nu(\{m_n/k\}e^{ky}) \right\} \\ & \times \sum_{l=0}^{\infty} \sum_{m=-l}^l \left\{ \sum_{i=1}^7 P_i^{(nlm)}(t, r) \mathcal{P}_{\alpha\beta}^{(i)lm}(\theta, \phi) \right. \\ & \left. + \sum_{i=1}^3 A_i^{(nlm)}(t, r) \mathcal{A}_{\alpha\beta}^{(i)lm}(\theta, \phi) \right\}. \end{aligned} \quad (27)$$

Here the first part is the contribution from extra dimensions, while the four dimensional effects have been divided into polar and axial perturbations respectively. The first seven are the polar perturbations, while the last three are the axial ones. As already emphasised earlier, these two contributions do not mix and hence one can treat them separately. We have already provided the evolution equations for the master variables associated with the axial perturbation in Eq. (17) and Eq. (18), which we will solve next. The solution (or, evolution) can be obtained in two ways, by the calculation of quasi-normal modes, or, performing a fully numerical Cauchy evolution of the initial data. We have performed both these analysis in this work and shall present the calculation of quasi-normal modes in the next section before taking up the Cauchy evolution of initial data.

TABLE III: Real and Imaginary parts of the quasi-normal mode frequencies have been presented. These are obtained from the *brane based approach* with the following choice of parameters associated with the extra dimensions: $d/\ell = 20; 1/\ell = 6 \times 10^7$. In particular, results for the first two Kaluza-Klein mass modes have been presented for four different choices of the angular momentum.

$m = 0.44, l = 2$			$m = 0.83, l = 2$	
Mode	Real	Imaginary	Real	Imaginary
j=1	0.467	-0.051	0.396	-0.038
j=2	0.530	-0.071	0.543	-0.104
j=3	0.378	-0.197	0.183	-0.168
j=4	0.473	-0.239	0.243	-0.369
$m = 0.44, l = 3$			$m = 0.83, l = 3$	
j=1	0.653	-0.078	0.843	-0.051
j=2	0.708	-0.084	0.708	-0.134
j=3	0.618	-0.244	0.773	-0.176
j=4	0.562	-0.437	0.576	-0.327
$m = 0.44, l = 4$			$m = 0.83, l = 4$	
j=1	0.847	-0.086	0.951	-0.064
j=2	0.827	-0.263	0.960	-0.219
j=3	0.791	-0.451	0.896	-0.393
$m = 0.44, l = 5$			$m = 0.83, l = 5$	
j=1	1.043	-0.090	1.123	-0.076
j=2	1.084	-0.272	-1.098	-0.233
j=3	1.002	-0.460	1.051	-0.404

IV. THE SPECTRUM OF ASSOCIATED QUASI-NORMAL MODES

In this section we will investigate the characteristic frequencies, namely the quasi-normal modes associated with the propagation of massive Kaluza-Klein modes in the Schwarzschild geometry induced on the brane hypersurface. This is usually performed by going over to the frequency space, such that,

$$u_{n,l}(t, r) = \int d\omega e^{-i\omega t} \psi_{n,l}(\omega, r) , \quad (28)$$

$$v_{n,l}(t, r) = \int d\omega e^{-i\omega t} \phi_{n,l}(\omega, r) . \quad (29)$$

At this stage all possible frequencies are allowed, but as we will see later on, this is not the case. Only some specific set of frequencies are allowed, known as the quasi-normal mode frequencies and hence the above integral will be converted to a sum over all the quasi-normal mode frequencies. The single most important fact about this expansion is that the quasi-normal mode frequencies can be imaginary. Since we do not expect any runaway situations associated with this problem, thus $\text{Im}(\omega) < 0$ are the allowed quasi-normal mode frequencies [64, 97–105]. Before getting into the details of obtaining the quasi-normal mode frequencies in this context, let us briefly discuss about another prediction of Eq. (17) and Eq. (28), namely late time wave tails. Since quasi-normal mode frequencies have a real as well as imaginary parts, it is exponentially suppressed and at late times ($t \rightarrow \infty$) it produces vanishing contribution. Therefore the wave tail, originating from existence of branch cut in the frequency integral of Eq. (28) dominates the late time behaviour of the gravitational perturbation $u_{n,l}(t)$. It turns out that the power law scaling of the perturbation modes have a universal behaviour. In particular, for massive gravitational modes, which includes the scenario presented in this work, the late time behaviour essentially corresponds to the following universal power law behaviour $u_{n,l}(t) \sim t^{-5/6} \sin(\omega t)$. Here the oscillation frequency ω depends on the mass of the perturbation mode linearly. Thus the late time behaviour is essentially governed by the $t^{-5/6}$ universal factor. We will need this fact in the later parts of this work. For the moment being we will exclusively concentrate on the quasi-normal mode analysis.

In order to determine the quasi-normal mode frequencies one also needs to impose suitable boundary conditions

TABLE IV: Real and Imaginary parts of the first few quasi-normal mode frequencies have been depicted. These values are obtained starting from the *brane based approach*, with the following choices of the extra dimensional parameters: $d/\ell = 30$; $1/\ell = 1.3 \times 10^{12}$. Results have been presented for two lowest lying Kaluza-Klein mass modes and for four choices of angular momentum associated with each modes.

$m = 0.43, l = 2$			$m = 0.82, l = 2$	
Mode	Real	Imaginary	Real	Imaginary
j=1	0.462	-0.053	0.702	-0.006
j=2	0.527	-0.072	0.385	-0.041
j=3	0.377	-0.201	0.541	-0.109
j=4	0.471	-0.241	0.253	-0.326
$m = 0.43, l = 3$			$m = 0.82, l = 3$	
j=1	0.650	-0.079	0.796	-0.036
j=2	0.616	-0.246	0.705	-0.138
j=3	0.679	-0.261	0.770	-0.179
j=4	0.562	-0.439	0.576	-0.331
$m = 0.43, l = 4$			$m = 0.82, l = 4$	
j=1	0.846	-0.086	0.948	-0.065
j=2	0.826	-0.264	0.906	-0.204
j=3	0.790	-0.452	0.833	-0.373
$m = 0.43, l = 5$			$m = 0.82, l = 5$	
j=1	1.041	-0.090	1.120	-0.076
j=2	1.027	-0.272	1.095	-0.234
j=3	1.001	-0.461	1.050	-0.406

on the solution space. These are — (a) the quasi-normal mode must be ingoing at the black hole horizon and (b) these modes must be outgoing in the asymptotic regions. These conditions are best suited in terms of the tortoise coordinate r_* , defined as integral of $\{dr/f(r)\}$, in which the horizon corresponds to $r_* \rightarrow -\infty$, while the asymptotic region implies $r_* \rightarrow \infty$. Thus the condition that quasi-normal modes are ingoing at the horizon implies that $u_{n,l}(\omega, r_*)$ as well as $v_{n,l}(\omega, r_*)$ behave as $\exp(-i\omega r_*)$ in the near horizon regime. A similar situation will exist for the asymptotic region as well. These boundary conditions will dictate the discrete values of the frequencies associated with the quasi-normal modes. These values will have three indices, the Kaluza-Klein mode index n , the angular momentum index l and the quasi-normal mode index p . Having obtained the corresponding quasi-normal modes one can substitute them back to Eq. (28) and Eq. (29) respectively and thus obtain the time evolution of the both $u_{n,l}(t, r_*)$ and $v_{n,l}(t, r_*)$. These estimates can then be compared with the Cauchy evolution problem and a match between the two will ensure correctness of our method presented here. Thus for completeness and consistency we will also present results for Cauchy evolution in the next section. We will mainly content ourselves with the continued fraction method but will briefly discuss the forward integration scheme as well.

A. Continued fraction method

The frequency spectrum associated with the quasi-normal modes can be obtained by starting with a suitable ansatz for $u_{n,l}(t, r)$ and $v_{n,l}(t, r)$ respectively. Given this ansatz one can try to obtain a power series solution associated with the differential equations presented in Eq. (17) and Eq. (18), resulting in recursion relation between the coefficients of various terms in the power series. This recursion relation will be satisfied provided the quasi-normal mode frequencies

TABLE V: In this table we have presented numerical estimates for real and imaginary parts of the quasi-normal mode frequencies obtained from the *bulk based approach*. The parameters characterising the bulk spacetime corresponds to: $d/\ell = 20$; $1/\ell = 6 \times 10^7$. In this situation as well we have presented the quasi-normal mode frequencies for four possible choices of angular momentum given the two lowermost Kaluza-Klein mode masses.

$m = 0.47, l = 2$			$m = 0.87, l = 2$	
Mode	Real	Imaginary	Real	Imaginary
j=1	0.480	-0.046	0.437	-0.015
j=2	0.540	-0.067	0.542	-0.087
j=3	0.381	-0.185	0.119	-0.128
j=4	0.477	-0.231	0.242	-0.318
$m = 0.47, l = 3$			$m = 0.87, l = 3$	
j=1	0.660	-0.076	0.862	-0.045
j=2	0.716	-0.082	0.719	-0.117
j=3	0.623	-0.239	0.785	-0.163
j=4	0.564	-0.431	0.576	-0.313
$m = 0.47, l = 4$			$m = 0.87, l = 4$	
j=1	0.853	-0.085	1.010	-0.067
j=2	0.831	-0.259	0.920	-0.193
j=3	0.793	-0.447	0.840	-0.359
$m = 0.47, l = 5$			$m = 0.87, l = 5$	
j=1	1.047	-0.089	1.176	-0.077
j=2	1.032	-0.269	1.108	-0.227
j=3	1.004	-0.457	1.058	-0.396

are discrete. For this purpose we start with the following general form of the coupled differential equations,

$$\begin{aligned}
-\frac{\partial^2 u_{n,l}}{\partial t^2} + \frac{\partial^2 u_{n,l}}{\partial r_*^2} - f(r) \left(m_n^2 + \frac{l(l+1)r-6}{r^3} \right) u_{n,l} \\
- f(r) \frac{m_n^2}{r^3} v_{n,l} = 0,
\end{aligned} \tag{30}$$

$$\begin{aligned}
-\frac{\partial^2 v_{n,l}}{\partial t^2} + \frac{\partial^2 v_{n,l}}{\partial r_*^2} - f(r) \left(m_n^2 + \frac{l(l+1)}{r^2} \right) v_{n,l} \\
- 4f(r)u_{n,l} = 0,
\end{aligned} \tag{31}$$

where $f(r) = 1 - (2/r)$. Subsequently eliminating derivatives with respect to r_* in favour of r and writing down the two master variables $u_{n,l}(t, r)$ and $v_{n,l}(t, r)$ as in Eq. (28) and Eq. (29) we obtain after simplifications,

$$\begin{aligned}
r(r-2) \frac{d^2 \psi_{n,l}}{dr^2} + 2 \frac{d\psi_{n,l}}{dr} + \frac{\omega^2 r^3}{r-2} \psi_{n,l} \\
- \left[m_n^2 r^2 + l(l+1) - \frac{6}{r} \right] \psi_{n,l} - \frac{m_n^2}{r} \phi_{n,l} = 0,
\end{aligned} \tag{32}$$

$$\begin{aligned}
r(r-2) \frac{d^2 \phi_{n,l}}{dr^2} + 2 \frac{d\phi_{n,l}}{dr} + \frac{\omega^2 r^3}{r-2} \phi_{n,l} \\
- [m_n^2 r^2 + l(l+1)] \phi_{n,l} - 4r^2 \psi_{n,l} = 0.
\end{aligned} \tag{33}$$

Having derived the basic equations governing $\psi_{n,l}$ and $\phi_{n,l}$ one normally writes down both these master variables in terms of various powers of r and $(r-2)$, such that the boundary conditions at horizon and at asymptotic regions can be satisfied. Subsequently the remaining pieces of $\psi_{n,l}$ and $\phi_{n,l}$ are solved by using the power series method. The resulting recursion relation between the coefficients of these power series will also be coupled and it is only helpful to combine them into a single matrix equation with off-diagonal entries illustrating the coupling between the systems.

TABLE VI: Real and Imaginary parts of the quasi-normal mode frequencies have been depicted in a bulk spacetime with the following set of parameters: $d/\ell = 30$; $1/\ell = 1.2 \times 10^{12}$ in the *bulk based approach*. The values have been presented for four choices of angular momentum, given the two lowest lying Kaluza-Klein modes.

$m = 0.43, l = 2$			$m = 0.79, l = 2$	
Mode	Real	Imaginary	Real	Imaginary
j=1	0.462	-0.053	0.672	-0.006
j=2	0.527	-0.072	0.456	-0.014
j=3	0.377	-0.201	0.542	-0.087
j=4	0.471	-0.241	0.534	-0.123
$m = 0.43, l = 3$			$m = 0.79, l = 3$	
j=1	0.650	-0.079	0.825	-0.055
j=2	0.616	-0.246	0.696	-0.149
j=3	0.678	-0.261	0.761	-0.187
j=4	0.562	-0.439	0.666	-0.377
$m = 0.43, l = 4$			$m = 0.79, l = 4$	
j=1	0.846	-0.086	0.937	-0.067
j=2	0.826	-0.264	0.898	-0.210
j=3	0.790	-0.452	0.829	-0.382
$m = 0.43, l = 5$			$m = 0.79, l = 5$	
j=1	1.041	-0.090	1.112	-0.078
j=2	1.027	-0.272	-1.089	-0.238
j=3	1.001	-0.461	1.045	-0.411

Performing the same for the master variables involved here as well, one ends up with the following matrix equation for $j > 0$, with integer j as,

$$\mathbf{P}_j \mathbf{V}_{j+1} + \mathbf{Q}_j \mathbf{V}_j + \mathbf{R}_j \mathbf{V}_{j-1} = 0. \quad (34)$$

Here, the coefficients \mathbf{P}_j , \mathbf{Q}_j and \mathbf{R}_j depend on the details of the system, i.e., on the parameters involved. The vector \mathbf{V}_j on the other hand corresponds to a column matrix constructed out of the power series coefficients for $\psi_{n,l}$ and $\phi_{n,l}$, such that one obtains

$$\begin{aligned} \mathbf{P}_j &= \begin{pmatrix} \alpha_j & 0 \\ 0 & \alpha_j \end{pmatrix}, \quad \mathbf{Q}_j = \begin{pmatrix} \beta_j + 3 & -\frac{m_n^2}{2} \\ -4 & \beta_j \end{pmatrix}, \\ \mathbf{R}_j &= \begin{pmatrix} \gamma_j - 3 & \frac{m_n^2}{2} \\ 0 & \gamma_j \end{pmatrix}, \end{aligned} \quad (35)$$

where the unknown coefficients α_j , β_j and γ_j can be written in terms of the Kaluza-Klein mode mass and the quasi-normal mode frequency ω as,

$$\begin{aligned} \alpha_j &= (j+1)(j+1-4i\omega), \\ \gamma_j &= \left(j-1 + \frac{(\omega-i\lambda)^2}{\lambda}\right) \left(j+1 + \frac{(\omega-i\lambda)^2}{\lambda}\right), \\ \beta_j &= -2j^2 + \left(-2 + \frac{8i\omega\lambda - 2\omega^2 + 6\lambda^2}{\lambda}\right)j \\ &\quad - l(l+1) + \frac{1}{\lambda} \left(3\lambda^2 - \omega^2 - 12i\omega\lambda^2 - 4\lambda^3 \right. \\ &\quad \left. + 4i\omega\lambda + 12\lambda\omega^2 + 4i\omega^3\right). \end{aligned} \quad (36)$$

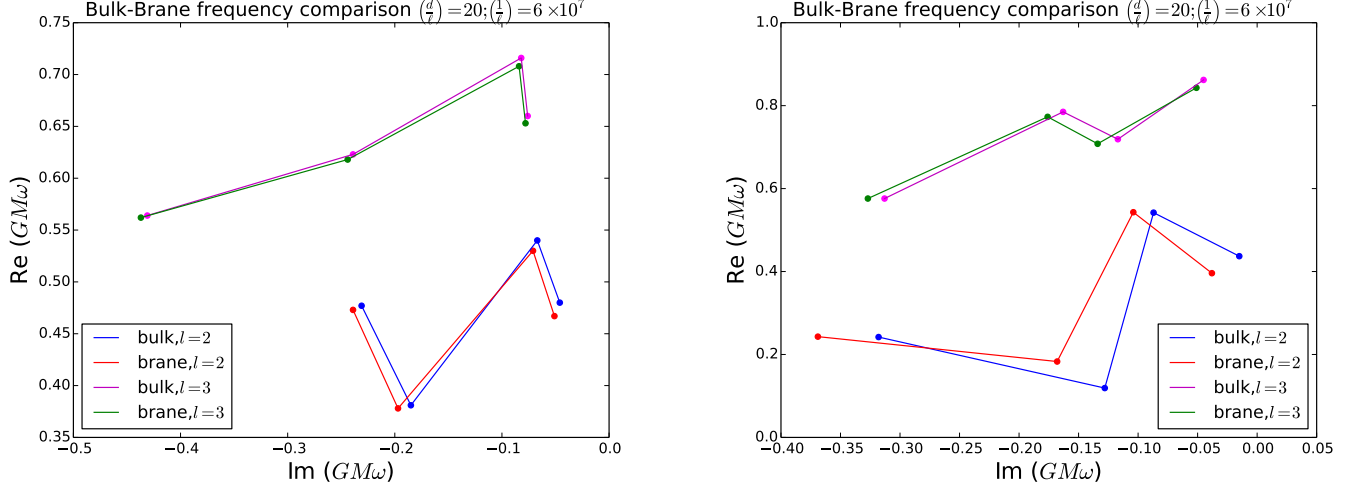


FIG. 1: Real and imaginary parts of the quasi-normal mode frequencies have been plotted. The figure on the left corresponds to the quasi-normal mode frequencies associated with the lowest lying Kaluza-Klein mass modes in both the brane and bulk based approach. The curves at the bottom shows the $l = 2$ case, while the curves at the top depicts the situation when $l = 3$. The figure to the right illustrates an identical situation but for the next Kaluza-Klein mass modes. As evident from the curves, the imaginary part of quasi-normal mode frequencies are smaller in the case of bulk based approach resulting in less damping. We will confirm this behaviour in the later sections.

where, $\lambda = \sqrt{m_n^2 - \omega^2}$. The above recursion relation must be supplemented with the zeroth order recursion relation, which simply reads, $\mathbf{P}_0 \mathbf{V}_1 + \mathbf{Q}_0 \mathbf{V}_0 = 0$. Given this one can use Eq. (34) to replace \mathbf{V}_1 in terms of \mathbf{V}_0 and \mathbf{V}_2 . Subsequently one can again replace \mathbf{V}_2 by higher order terms using Eq. (34) repeatedly. This method of solving the matrix valued recursion relation presented in Eq. (34) is known as the method of continued fraction. In this method, following the procedure outlined above one ends up with an equation of the form $\mathbf{M} \mathbf{V}_0 = 0$, where the matrix \mathbf{M} reads,

$$\mathbf{M} = \mathbf{Q}_0 - \mathbf{P}_0 [\mathbf{Q}_1 - \mathbf{P}_1 \{\mathbf{Q}_2 + \mathbf{P}_2 \mathbf{M}_2\} \mathbf{R}_2]^{-1} \mathbf{R}_1. \quad (37)$$

Here \mathbf{M}_j is a matrix which can be written in terms of \mathbf{P}_{j+1} , \mathbf{Q}_{j+1} , \mathbf{R}_{j+1} and most importantly also depends on \mathbf{M}_{j+1} . Moreover the matrix \mathbf{M}_j when acts on \mathbf{V}_j yields \mathbf{V}_{j+1} . Thus in order for the matrix equation $\mathbf{M} \mathbf{V}_0 = 0$ to have non-trivial solutions for \mathbf{V}_0 , one must have

$$\det \mathbf{M} = 0. \quad (38)$$

In principle one needs to take into account an infinite number of terms to solve the above equation. However in practice one truncates \mathbf{M}_j at some order J , and hence obtain all the lower order matrices starting from \mathbf{M}_J . Of course, at a later stage one needs to check the independence of the solution of Eq. (38) explicitly on the truncation order J . We have solved the above matrix valued recursion relation using the continued fraction method discussed earlier in the symbolic manipulation package MATHEMATICA and have obtained the corresponding lowest lying quasi-normal mode frequencies associated with various Kaluza-Klein mode masses for different values of angular momentum. These values are listed in four tables. In Table III we present both the real and imaginary parts of the quasi-normal mode frequencies for the two lowest lying Kaluza-Klein mass modes associated with the following values: $d/\ell = 20; 1/\ell = 6 \times 10^7$. It is clear that as the mass increases the imaginary part of the lowest quasi-normal mode frequency decreases, while it increases with angular momentum. For example, when $l = 2$, $\text{Im } \omega = -0.05$ for $m_1 = 0.44$, while it becomes -0.04 as the mass increases to $m_2 = 0.83$. Hence more massive the Kaluza-Klein modes are, the quasi-normal mode functions are less and less damped — a feature in complete agreement with the result of [68]. While for $m = 0.44$, the imaginary part of the lowest quasi-normal mode frequency will read $\text{Im } \omega = -0.051$ for $l = 2$, while it becomes -0.078 as the angular momentum increases to $l = 3$. Thus with an increase of angular momentum the imaginary part of the quasi-normal mode frequency also increases. Hence among the modes with $l = 2$ and $l = 3$, the time evolution of the $l = 3$ mode will be more damped in comparison to the $l = 2$ one. This feature is also present in Table IV, where the quasi-normal mode frequencies have been presented for a different choice of the ratio between brane separation and bulk curvature scale, namely for $d/\ell = 30$ and $1/\ell = 1.3 \times 10^{12}$.

These numerical values are again chosen to be consistent with previous experimental bounds on d and ℓ as explained earlier. In this case also as the mass of the Kaluza-Klein mode increases the imaginary part of the quasi-normal mode

frequency decreases, while the increase of angular momentum has a reverse effect. For the same choices of the bulk parameters, the Kaluza-Klein mode masses for the brane based and the bulk based approach differs as evident from [Table I](#) and [Table II](#). For example, in the situation where $d/\ell = 20$; $1/\ell = 6 \times 10^7$, the lowest lying Kaluza-Klein mode mass in brane based approach is $m_1 = 0.44$, while that in the bulk based approach being $m_1 = 0.47$. Hence the imaginary part of the quasi-normal mode frequency will be lower for the bulk based approach. This has interesting implications — the axial perturbation generated from bulk Einstein's equations will decay in a slower pace in time when compared to the corresponding perturbation mode originated from effective field equations on the brane. This situation has been clearly depicted in [Table V](#) and [Table VI](#) respectively (see also [Fig. 1](#)). One can also check that the quasi-normal mode frequencies derived here indeed matches with those derived in the direct integration scheme which we will discuss next.

B. Direct integration method

In the previous section we have discussed one particular method of determining the quasi-normal mode frequencies associated with the perturbation of brane world black hole. However for completeness we present another supplementary method of computing the quasi-normal mode frequencies, which can be used along with the continued fraction method to correctly predict the quasi-normal mode frequencies. In this method, as the name suggests, one integrates directly from the horizon to the asymptotic region given the boundary conditions mentioned earlier. In this problem we have two master variables characterising the axial gravitational perturbation and satisfying two second order coupled ordinary differential equations (see [Eq. \(B5\)](#) and [Eq. \(B6\)](#) respectively in [Appendix B](#)). The solution in the near horizon regime will have $e^{-i\omega r_*}$ times a power series around the horizon, while at infinity it will behave as $e^{-k_\infty r_*}$, where k_∞ is the wave number in the asymptotic region. The asymptotic solution will be characterised by a two-dimensional column vector $\{b_\infty^{(1)}, b_\infty^{(2)}\}$, for which one can choose a suitable orthonormal system of basis vectors. Numerical integration of these differential equations from the horizon out to infinity will lead to a (2×2) matrix $\mathbf{S}(m_n, \omega)$, which can be expanded in the basis introduced above. Finally, setting the determinant of this matrix \mathbf{S} to zero one can solve for the quasi-normal mode frequencies [\[101, 103\]](#).

Further note that, this method is particularly suited for determination of quasi-bound states, for which the leading order behaviour of the fields at infinity is well understood. However for the determination of quasi-normal mode frequencies one needs to extract additional, sub-dominant behaviour of the mode functions at infinity, which makes this approach prone to numerical errors. However if the imaginary part is small compared to the real part, one can determine the quasi-normal mode frequencies to sufficient accuracy. In practice one integrates these differential equation to some high value of radial distance and the result must be impermeable to any shift in this distance. Also one can supplement one of these methods by checking whether for a given Kaluza-Klein mode mass and angular momentum one obtains the same quasi-normal mode frequency from the other. We have explicitly checked that this is indeed the case, the values obtained from the continued fraction method is in good agreement with those obtained from the direct integration scheme as well. This depicts the internal consistency of our model in a straightforward manner.

V. NUMERICAL ANALYSIS OF THE QUASI-NORMAL MODES

The principal aim of this work was to determine the time evolution of the perturbations obtained from the effective gravitational field equations on the brane. Also, to contrast the same with the time evolution of perturbation derived from bulk Einstein's equations. One can achieve this by following two possible avenues — (a) Obtaining the quasi-normal mode frequencies and hence obtaining the time evolution and (b) Solving the Cauchy evolution problem numerically and hence arrive at the evolution of the gravitational perturbation.

In this section we will follow the first method where the time evolution of the mode function $u_{n,l}(t)$ depicting axial gravitational perturbation will be presented, using the quasi-normal mode analysis performed in [Section IV](#). For this purpose we will use [Eq. \(28\)](#), where the integral over all frequencies will now be replaced by summation over all the quasi-normal mode frequencies. Thus our strategy will be as follows, we will use the numerically computed quasi-normal mode frequencies and then sum over them in order arrive at the time evolution for the mode function $u_{n,l}(t)$. Here we would like to reiterate the fact that n stands for the Kaluza-Klein modes and l is the angular momentum associated with the gravitational perturbation. For example, $u_{0,2}$ corresponds to the axial gravitational perturbation associated with angular momentum $l = 2$ around a general relativity solution, while $u_{1,3}$ is the axial gravitational perturbation associated with the lowest lying Kaluza-Klein mode and with angular momentum $l = 3$. In what follows using the numerical values of quasi-normal mode frequencies we will present time evolution of $u_{n,l}(t)$ for a few low

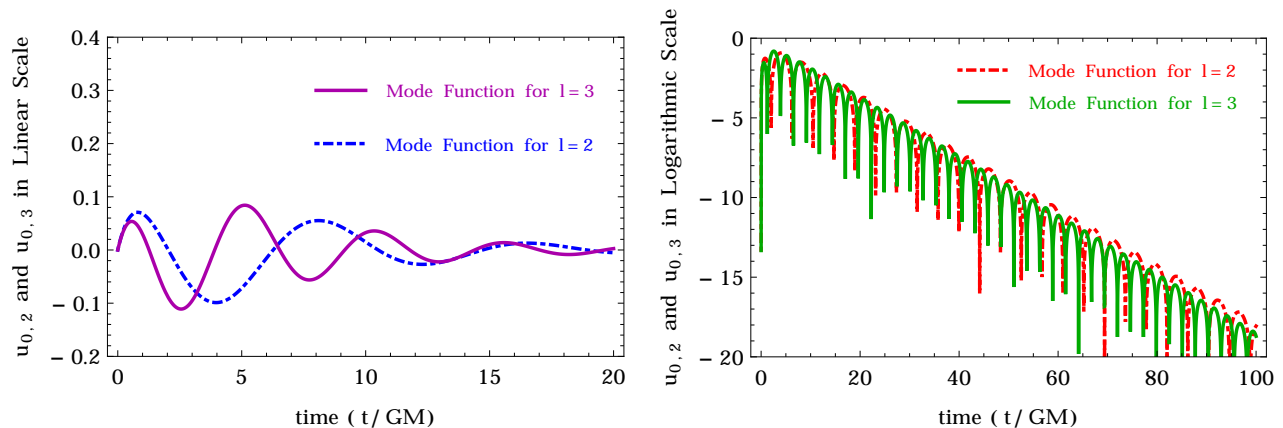


FIG. 2: Time evolution of the master mode function $u_{n,l}(t)$ associated with axial gravitational perturbation for two different values of angular momentum l in the context of general relativity have been depicted. The time scale has been normalised to the mass of the central hole, i.e., $t \rightarrow t/GM$. Moreover the figure in the left illustrates the actual evolution of the mode function with time, while the right one presents the same but in a Logarithmic scale. The amplitude of the mode function corresponding to $l = 3$ is slightly smaller compared to the mode function having $l = 2$, as evident from the right figure. In both of them the dotted one stands for mode function with $l = 2$, while the continuous one is the mode function with $l = 3$. We will contrast this scenario with the respective ones in the presence of extra dimensions.

lying Kaluza-Klein modes with different choices of angular momentum l . These will be contrasted with the mode functions $u_{0,l}$ associated with general relativity.

Note that this process is inherently approximate, since in principle one should add all the quasi-normal mode frequencies in order to obtain the time evolution of the perturbation, while here we will consider a few lowest lying quasi-normal modes to perform the same. Even though this is certainly an approximate description, it will nevertheless provide the overall behaviour of the gravitational perturbation with time and the key features that will distinguish the scenario presented here from that in general relativity. More refined results can be obtained using the Cauchy evolution, which we will present in the next section. This will provide another self-consistency check of our formalism and hence of the associated results.

As a first step towards the same we will present the time evolution of the axial perturbation in the context of general relativity alone. This will set the stage for what to come next. This has been presented in Fig. 2, where we have depicted how the mode functions evolve with time in the actual scale as well as in the Logarithmic scale. The advantage of the Logarithmic scale is that, it can enhance very tiny differences, while the disadvantage being, it will make large differences to appear as a small one. The left figure in Fig. 2 presents the actual time evolution of the $l = 2$ and $l = 3$ mode functions in general relativity, i.e., $u_{0,2}(t)$ and $u_{0,3}$ respectively, while the right one presents the same in Logarithmic scale. It is clear that there is appreciable difference between the two at earlier times, which gets washed out as the modes gradually decay down. On the other hand the Logarithmic plot shows exactly the opposite nature as explained earlier.

Returning back to our main goal, we have illustrated time variation of the perturbation associated with the lowest lying Kaluza-Klein mode having mass $m_1 = 0.44$ and have contrasted the same with general relativity in Fig. 3. The figures on the left depict time variation of the perturbation for $l = 2$ in both actual and Logarithmic scale, while those on the right are for $l = 3$. The main difference emerging from Fig. 3 is that the damping time scale of the massive modes are much greater compared to those in general relativity. The same is true for the Logarithmic plots as well, where the fact that modes in general relativity are heavily damped in comparison to the massive modes is much pronounced. The features of the massive modes remain identical as one considers the second lowest Kaluza-Klein mode having mass $m_2 = 0.83$ as well. Here also the slower decay of the massive modes with time is the key distinguishing feature between general relativity and the higher dimensional model discussed here.

So far we have been discussing the time evolution of the gravitational perturbation starting from the effective gravitational field equations on the brane. At this stage let us try to understand the corresponding situation when the gravitational perturbation originating from the bulk Einstein's equations is being considered. As emphasised earlier this will be similar to the brane based approach but will have an associated Kaluza-Klein mass mode, which will be different. For example, as evident from Table I and Table II for the same choice of bulk parameters, i.e., $d/\ell = 20$; $1/\ell = 6 \times 10^7$, the Kaluza-Klein mass spectrum will be different in the two scenarios. Thus in Fig. 4 we have presented the time evolution of the gravitational perturbation derived from the bulk based approach. Here also we observe the same key features, e.g., very slow decay of the perturbation in contrast to that in general relativity. Thus if the

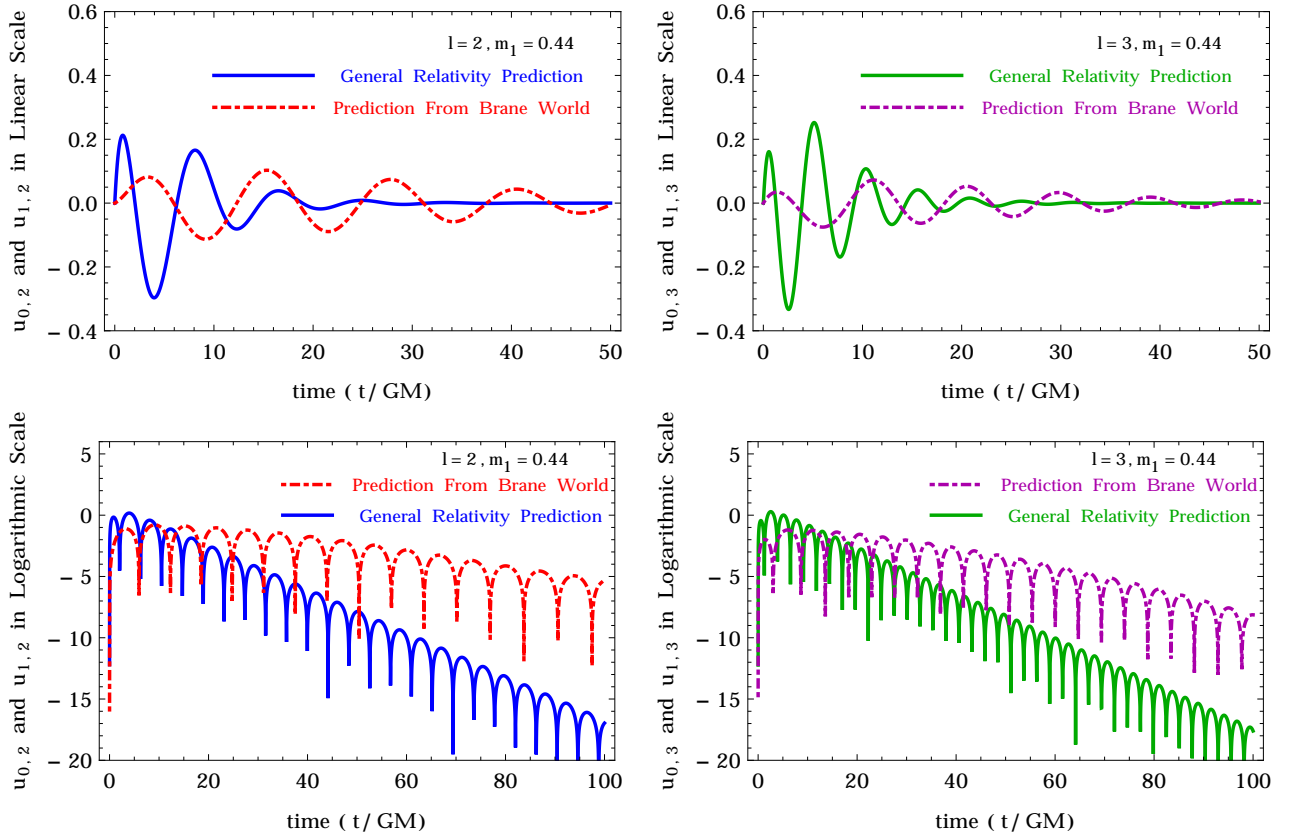


FIG. 3: Time evolution of the master mode function $u_{n,l}(t)$ for two different values of angular momentum both in the context of general relativity ($n = 0$) as well as in the *brane based approach* have been presented. All the figures are associated with the lowest lying Kaluza-Klein mode mass $m_1 = 0.44$ (see Table I) but for two different choices of the angular momentum. For brevity we have presented both — (a) the figures have been drawn in a Logarithmic scale (in the below panel) and (b) the figures in actual scale (in the top panel). All these figures clearly bring out the key differences between these two scenarios. See text for more discussions.

ring down phase of any black hole merger is being probed to intermediate times, where the evolution of gravitational perturbation is still dominated by the quasi-normal modes, any departure from the general relativity prediction can possibly signal the existence of extra spacetime dimensions. Following the general trend, in Fig. 4 as well we have presented the time evolution in actual as well as in Logarithmic scale for two possible choices of angular momentum $l = 2$ and $l = 3$ respectively.

This enables one to compare the bulk and the brane based approach given the same bulk parameters. The resulting discord should be attributed to the difference between the masses of the respective Kaluza-Klein modes. As evident from Fig. 5 this difference is really very small unlike the situation with general relativity. Moreover since the masses of the Kaluza-Klein modes are higher in the bulk based approach they would decay slower. This can be clearly seen from both the Logarithmic plots in Fig. 5, where the perturbation in the bulk based approach becomes larger than the brane based one at late times. Same features appear for both the angular momenta as well, however the difference is much smaller in higher angular momentum compared to the lower one.

All these features can also be seen for the second lowest Kaluza-Klein mode mass, $m_2 = 0.87$, in the bulk based approach. The time evolution of the corresponding gravitational perturbation in both actual and Logarithmic scale for two choices of the angular momentum shows very similar features when compared with the lowest lying Kaluza-Klein mass mode. As expected, the massive modes decay much slowly in comparison with general relativity. Further from the comparison of brane and bulk based approach for the second lowest lying Kaluza-Klein mode, one may infer that the difference only becomes sensible after a large time has elapsed and hence if the ring down phase can be probed minutely at very late times one may infer the preference of the bulk based approach over the brane based one or vice versa. However, the situation is not so simple and another subtle effect comes into play at late times, which corresponds to the wave tail. All the quasi-normal modes are inherently exponentially suppressed and hence at very late times their effects are negligibly small. In this situation the wave tails enter the picture and in most of the cases

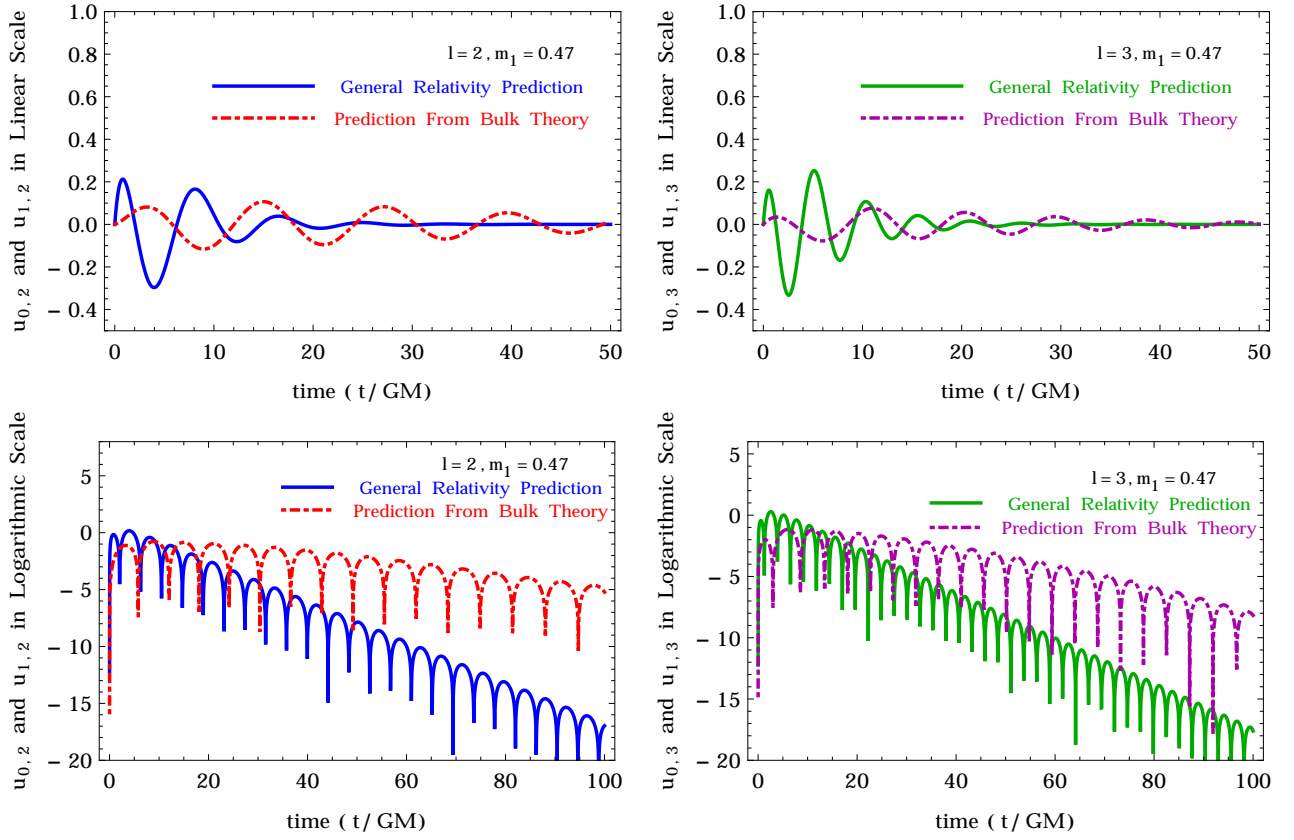


FIG. 4: The above figures depict the time evolution of the master mode function $u_{n,l}(t)$ in the *bulk based approach* and has been contrasted with that in general relativity ($n=0$). In this case also behaviour of the mode functions in a Logarithmic scale as well as in the actual scale have been presented. The Kaluza-Klein mode mass associated with the master variable presented here corresponds to the lowest one with $m_1 = 0.47$ with the following parameters: $d/\ell = 20$; $1/\ell = 6 \times 10^7$.

the late time behaviour is essentially governed by the wave tail decaying only as a power law (this is identical to the “bulk based approach” as well, see [70]). Since the scaling of the power law is mostly universal, independent of the nature of fields and mass of the fields under consideration, both the bulk and brane based approach will decay by an identical power law behaviour. This will make the detection of these two different approaches by late time measurements extremely difficult.

VI. CONSISTENCY OF THE APPROACH: COMPARISON WITH CAUCHY EVOLUTION

The previous section illustrates the methods to determine the quasi-normal mode frequencies, using which we have obtained the time evolution of the perturbation mode $u_{n,l}$. This is so because, in the limit of $m_n \rightarrow 0$ (i.e., general relativity limit) this mode represents the axial gravitational perturbation, while the other essentially becomes a gauge degree of freedom. Hence we can compare the time evolution of $u_{n,l}$ with the respective one in general relativity and see the harmony as well as possible discord among the two. We have already performed the same in the previous section. However in principle one expects the above approach to match with the Cauchy evolution of the perturbation equations presented in Eq. (B5) and Eq. (B6) respectively in Appendix B. This is what we will explore in this section.

For this purpose, we closely follow the analysis put forward in [65] but modifying it wherever necessary. Referring back to Eq. (17) and Eq. (18) as the key differential equations for the master variables, one can write them in a compact manner as

$$\mathcal{D}\Psi + \mathbf{V}(r)\Psi = 0. \quad (39)$$

Here, Ψ is a two dimensional column matrix constructed out of $u_{n,l}$ and $v_{n,l}$ respectively. Rather than working with the normal (t, r) coordinates it is instructive to transform to the light cone coordinates. The transformation into the

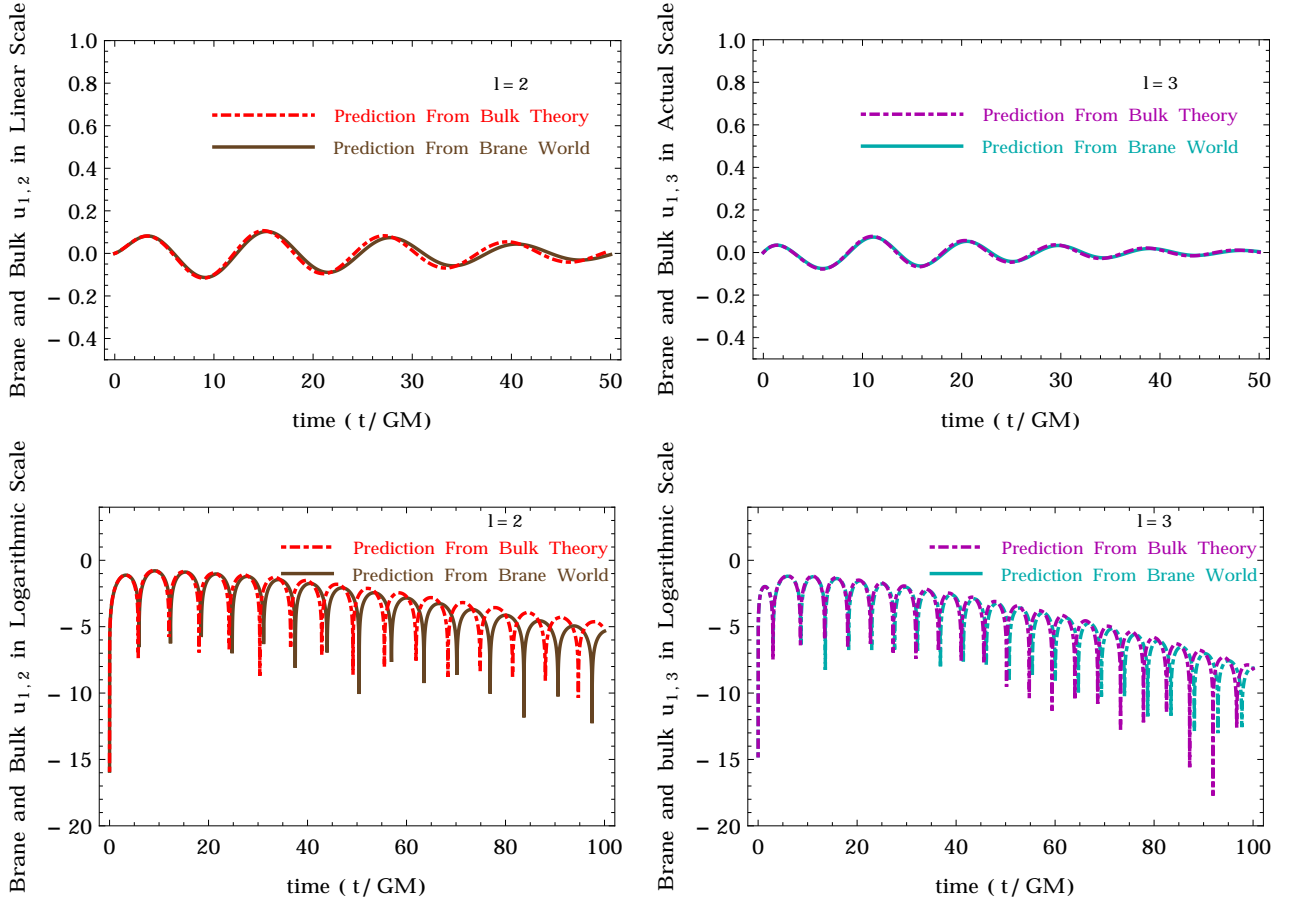


FIG. 5: The two scenarios presented in this work, namely the perturbation of effective four dimensional Einstein's equations or the perturbation of bulk Einstein's equations, have been illustrated in this figure. Both for the identical choice of the extra dimensional parameters, i.e., $d/\ell = 20$; $1/\ell = 6 \times 10^7$. It is clear that the time evolution of the mode function $u_{n,l}(t)$ differ from each other in these two distinct approaches. This is primarily due to the difference between the Kaluza-Klein mode masses in these two approaches. See text for more discussions.

light-cone coordinates can be achieved by introduction of the null coordinates as: $u = t - r_*$, $v = t + r_*$. Use of these null coordinates modifies Eq. (39) to

$$4\partial_u\partial_v\Psi + \mathbf{V}(u,v)\Psi = 0, \quad (40)$$

where

$$\Psi = \begin{pmatrix} u_{n,l} \\ v_{n,l} \end{pmatrix}, \quad \mathbf{V} = \begin{pmatrix} V_{11} & V_{12} \\ V_{21} & V_{22} \end{pmatrix}. \quad (41)$$

Here all the matrix coefficients of \mathbf{V} are dependent on the black hole solution on the brane and the Kaluza-Klein mode mass m_n .

For clarity, we have suppressed the functional dependence of the potential matrix \mathbf{V} for the time being. To proceed further we need to introduce a notion of time evolution operator. For this purpose, we note that for an arbitrary function of time $f(t)$, the function given by $e^{h\partial_t}$ is the time evolution operator, in the sense that $e^{h\partial_t}f(t) = f(t+h)$. Thus in order to obtain the time evolution of the mode functions Ψ , we apply the time evolution operator on Ψ . This yields,

$$\Psi(t+h) = e^{h\partial_t}\Psi = e^{h\partial_u+h\partial_v}\Psi. \quad (42)$$

Eq. (42) can be written in a nice manner by expanding the right hand side, resulting into,

$$\begin{aligned}
\Psi(u+h, v+h) &= \sum_{j=0} \frac{1}{j!} (h\partial_u)^j \sum_{k=0} \frac{1}{k!} (h\partial_v)^k \Psi(u, v) \\
&= \left[e^{h\partial_u} + e^{h\partial_v} - 1 + \frac{1}{2} h^2 \partial_u \partial_v \left(1 + \frac{h\partial_u}{2!} + \frac{h\partial_u^2}{3!} + \dots \right) \left(1 + \frac{h\partial_v}{2!} + \frac{h\partial_v^2}{3!} + \dots \right) \right] \Psi(u, v) \\
&= \left[e^{h\partial_u} + e^{h\partial_v} - 1 + \frac{1}{2} h^2 \partial_u \partial_v \left\{ \left(e^{h\partial_u} - (h\partial_u)^2 \left(\frac{1}{2!} - \frac{2}{3!} \right) - \dots \right) + \partial_u \rightarrow \partial_v \right\} \right] \Psi(u, v) \\
&= \left[e^{h\partial_u} + e^{h\partial_v} - 1 + \frac{1}{2} h^2 \partial_u \partial_v \{ (e^{h\partial_u} + \mathcal{O}(h^2)) + (e^{h\partial_v} + \mathcal{O}(h^2)) \} \right] \Psi(u, v) .
\end{aligned} \tag{43}$$

The last expression of Eq. (43) can be expanded immediately and hence finally we have,

$$\begin{aligned}
\Psi(u+h, v+h) &= \Psi(u+h, v) + \Psi(u, v+h) - \Psi(u, v) \\
&\quad - \frac{h^2}{8} \left\{ \mathbf{V}(u+h, v) \Psi(u+h, v) \right. \\
&\quad \left. + \mathbf{V}(u, v+h) \Psi(u, v+h) \right\} .
\end{aligned} \tag{44}$$

This can be thought of as an evolution equation in the light-cone coordinates u and v . The interesting aspect of this formalism is that once initial data is specified in the u, v coordinates, we need no additional boundary conditions, which is unlike the physical coordinates t, r (or, for that matter t, r_*). We evolve the system with Gaussian initial data in u and constant data in v . Fig. 6 illustrates the numerical evolution of Ψ as a function of time for different choices of the angular momentums and Kaluza-Klein mode masses obtained by numerically integrating the above evolution equation in light cone coordinates. Interestingly and as expected, it illustrates all the basic properties that we have already observed from a quasi-normal mode analysis. For example, in all the cases illustrated in Fig. 6 it is clear that at intermediate times (i.e., when the spectrum of quasi-normal modes dominate the evolution of gravitational perturbation) the mode functions due to massive Kaluza-Klein modes will dominate over those in general relativity. This is again due to the fact that the massive modes suffer much less damping compared to the respective ones in general relativity. The translation of the same in the quasi-normal mode language corresponds to the imaginary part of the quasi-normal mode frequency to be smaller for massive Kaluza-Klein modes compared to the modes in general relativity. Further the fact that as the mass of the Kaluza-Klein mode increases it experiences less and less damping is also borne out by both Cauchy evolution (see Fig. 6) and the quasi-normal mode analysis. Of course, there are minute differences present between both these methods, which have their origin in the initial conditions and the fact that the Cauchy evolution is more accurate compared to the quasi-normal mode analysis. All in all, the quasi-normal mode analysis and the Cauchy evolution of initial data provides a complete and consistent description of the time evolution of gravitational perturbation in presence of extra spatial dimensions.

Besides being consistent with the quasi-normal mode analysis, Cauchy evolution has more additional features to offer. The most important such feature is the presence of late time power law tail. Since at the intermediate stages, the contributions from quasi-normal mode dominates, the behaviour of the mode function $u_{n,l}(t)$ as presented in Fig. 6 resembles those in Section V. However, if one can perform the Cauchy analysis for a sufficiently long time, gradually the contributions from quasi-normal modes become smaller compared to the late time tail. Thus the Cauchy evolution of the initial data for a longer time must result in the desired power law tail and will serve as another consistency check of our approach. Following this we have presented a long time Cauchy evolution of the perturbation equation in Fig. 7, which distinctly depicts the late time wave tail. As evident from Fig. 7, the mode function is initially dominated by the quasi-normal modes and hence decays linearly in the Logarithmic scale. However in the late stages of Cauchy evolution the power law takes over and dominates the quasi-normal modes, thus presenting an almost constant-in-time behaviour of the same. Hence, the numerical analysis of the Cauchy evolution of the perturbation equation is completely consistent with theoretical expectation, providing one more consistency check of our formalism.

VII. DISCUSSION AND CONCLUDING REMARKS

In this work we set out to achieve three goals in a single framework — (a) Effect of extra spatial dimensions on the gravitational perturbation and whether one can provide some possible observational signatures of the same in the ring down phase of black hole merger; (b) How the two possible methods to determine the gravitational perturbation on

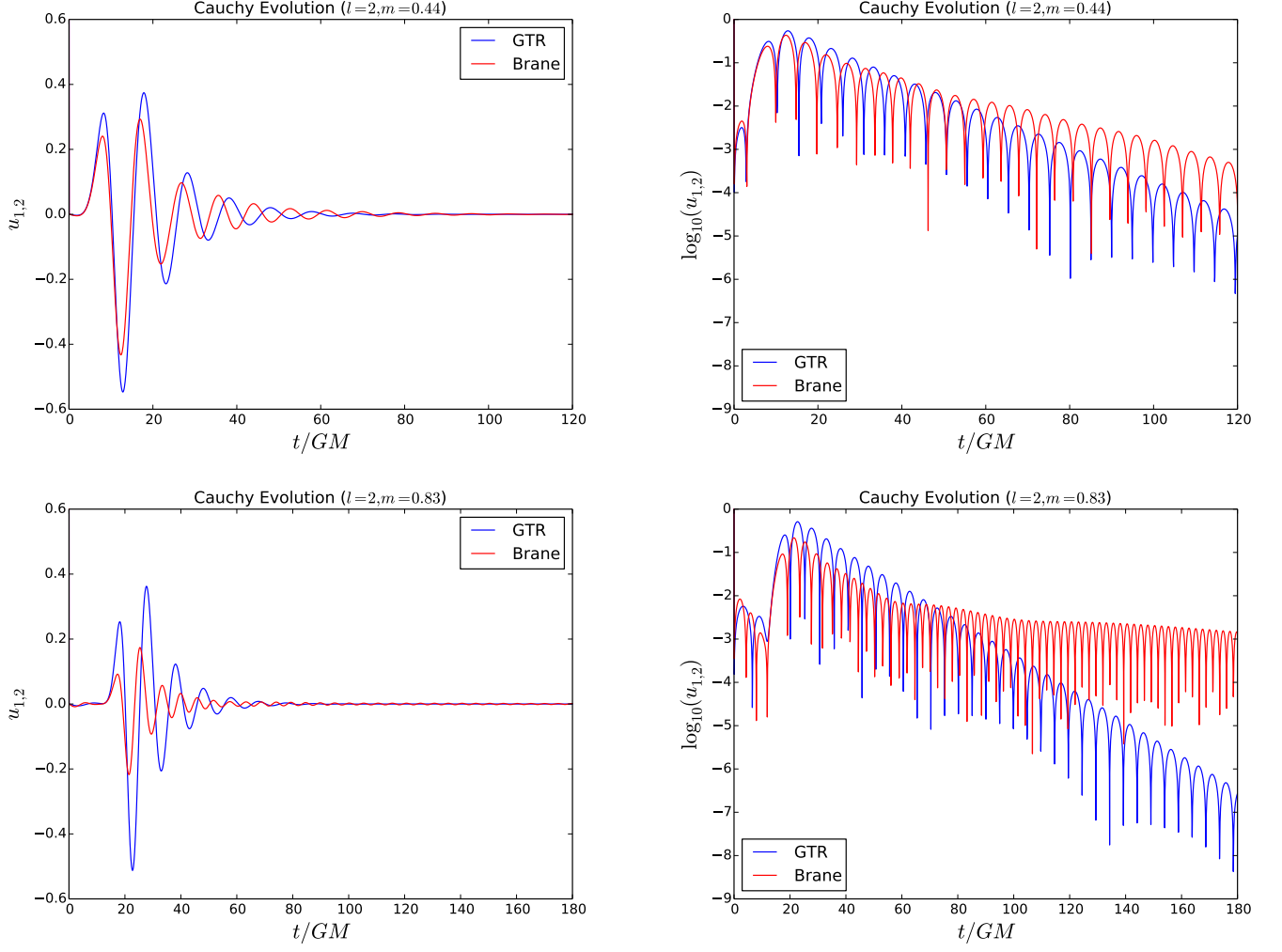


FIG. 6: The Cauchy evolution of the master variable $u_{n,l}(t)$ has been plotted for two different choices of the Kaluza-Klein mode masses for a given angular momentum. The figures in the top panel depicts the evolution of the master variable for $l = 2$ and $m_1 = 0.44$, the lowest lying Kaluza-Klein mode with $d/\ell = 20$ and $1/\ell = 6 \times 10^7$. The figure on the left is the actual variation of the master variable with time, while that on the right presents the same variation but in a Logarithmic scale. While the figures in the bottom panel illustrates the same, however for $l = 2$ and Kaluza-Klein mode mass $m_2 = 0.83$. It is clear that as the mass increases the master variable becomes less and less damped in comparison with general relativity. Further we clearly observe that the overall features present in the Cauchy evolution of the master variable are identical to those obtained by the quasi-normal mode analysis, illustrating the internal consistency of both the methods adapted here.

the brane, namely by either perturbing the bulk gravitational field equations or perturbing the *effective* gravitational field equations on the brane, differ as far as the behaviour of the gravitational perturbation is concerned; (c) Whether the analysis using quasi-normal modes is consistent with the fully numerical Cauchy evolution of the initial data. We believe to have addressed all of them in a satisfactory manner in this work which we summarise below.

We have explicitly demonstrated that the existence of extra spatial dimensions indeed modifies the gravitational perturbation equation by essentially introducing a tower of massive perturbation modes in addition to the standard massless one. Thus the presence of massive gravitational perturbation modes is a definitive signature of the existence of higher dimensions. To see the consequences of the above we have discussed the behaviour of quasi-normal modes in this context. In particular, we have shown that for the massive modes the imaginary part of the quasi-normal mode frequencies are much small compared to those in general relativity. This has resulted in the time evolution of the massive gravitational perturbations to exhibit a weak decay rate in comparison to the massless modes as in general relativity. The above phenomenon opens up the observational window to probe the possible existence of higher dimensions using gravitational wave observation. If the ring down phase during the merger of two black holes can be accurately measured for a sufficient amount of time (unlike the aLIGO measurements where the ring down phase

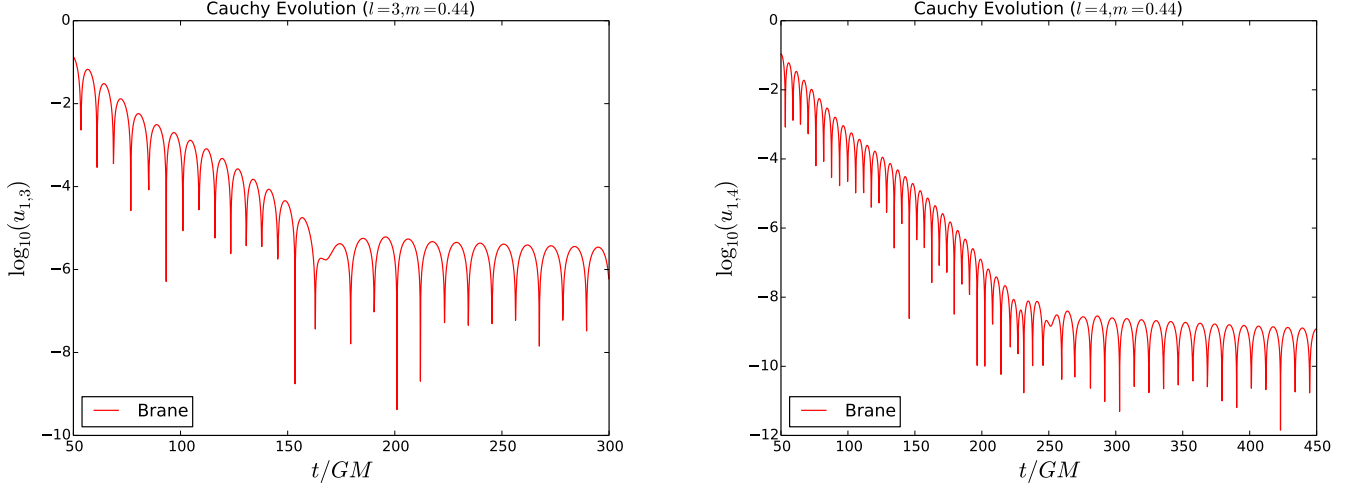


FIG. 7: The Cauchy evolution of the master variable $u_{n,l}(t)$ associated with the brane based approach has been plotted for two different choices of the angular momentum given a Kaluza-Klein mode mass to illustrate the late time behaviour. The figure in the left depicts the evolution of the master variable for $l = 3$ and $m_1 = 0.44$, the lowest lying Kaluza-Klein mode with $d/\ell = 20$ and $1/\ell = 6 \times 10^7$. The figure on the right is for $l = 4$ and identical Kaluza-Klein mode mass. It is clear that as time progresses the power law tail dominates over the exponential damping due to quasi-normal modes. This once again illustrates the consistency of Cauchy evolution with the theoretical methods adapted here.

was barely measured and is the one with large errors) there will definitely be departure from the general relativity prediction and thus it may lead to concrete observational signature for the existence of higher dimensions or it may provide stringent constraints on the associated parameters. This will become feasible as the sensitivity of the aLIGO detectors are further improved or the space based gravitational wave detector LISA becomes operational. We will address the detailed observational aspects of this particular signature of extra dimension in light of the recent detection of gravitational waves at aLIGO in a future work.

The evolution equation for the gravitational perturbation obtained by perturbing the bulk field equations has already been derived in [68], while in this work we have derived the evolution equation by perturbing the *effective* gravitational field equations on the brane hypersurface. From the structure of the equation itself, difference between these two approaches should be evident. In both the bulk based and the brane based approach the four dimensional perturbation equation looks identical with one crucial difference, namely, the masses associated with both the approaches are different. This is because the differential equation satisfied by the extra dimensional part are different in these two scenarios. This in turn leads to difference in the quasi-normal mode frequencies as evident from Fig. 1, the imaginary parts of the quasi-normal mode frequencies are smaller for the bulk based approach in comparison to the brane based one. Since the difference is small there is possibly no way in foreseeable future to observationally distinguish these two effects (see e.g., Fig. 5) however theoretically there does exist a difference between these approaches. Naively speaking, this is due to the fact that a solution of the *effective* gravitational field equation on the brane may not have any higher dimensional embedding.

Finally the time evolution of the gravitational perturbation can be obtained by either performing a quasi-normal mode analysis or by performing a fully numerical Cauchy evolution. We have performed both in this work and they are found to match very well with each other. This is expected as well as necessary for internal consistency of any gravitational perturbation computation. In particular from the quasi-normal mode analysis we have learned that the massive modes decay much slowly in contrast with the massless general relativity modes (see e.g., Fig. 3), which is also confirmed by the Cauchy evolution as well (see e.g., Fig. 6). Thus keeping aside minute details overall behaviour of the time evolution of gravitational perturbation is identical whether one performs a quasi-normal mode analysis or complete Cauchy evolution.

Having described the consistency of the time evolution obtained by using quasi-normal modes as well as a fully numerical Cauchy evolution of the perturbation equations, let us comment on possible detectability of the scenario presented above. For that purpose it is important to know the frequencies associated with the gravitational perturbation modes. The corresponding frequencies can broadly be divided into two classes, those originating from the real part of the quasi-normal modes of the gravitational perturbation and the universal one present in the very late time region [68, 103] originating from the power law tail. As far as the possible detectability of the scenario presented here in aLIGO-like detectors using the real parts of the quasi-normal modes is concerned, one can safely say that

TABLE VII: Frequencies (in Hz) of oscillation for the quasi-normal modes emanating from black holes having different masses have been depicted. Numerical estimates for the frequencies have been presented for general relativity as well as for the two lowest lying Kaluza-Klein modes with masses $m_1 = 0.43$ and $m_2 = 0.83$ respectively. It is also clear that the frequency of the modes increases with an increase in the l value. It is clear that as the mass of the black hole increases the frequency decreases. Thus more massive the black hole is it is more problematic to detect in aLIGO. While the Kaluza-Klein modes have better chance of originating if the mass of the black hole increases, this leads to lowering of the frequency and hence have less chance of getting detected in aLIGO.

Frequencies for $l = 2$			
(M/M_\odot)	General Relativity	KK Mode ($m_1 = 0.43$)	KK Mode ($m_2 = 0.82$)
1	24140	14930	12441
10	2414	1493	1244.1
10^2	241.4	149.3	124.4
10^3	24.1	14.9	12.4
10^4	2.4	1.5	1.2
10^5	0.2	0.1	0.1
Frequencies for $l = 3$			
1	38779	21328	27856
10	3877.9	2132.8	2785.6
10^2	387.7	213.3	278.6
10^3	38.7	21.3	27.8
10^4	3.9	2.1	2.8
10^5	0.3	0.2	0.3

most likely it is not a feasible option. This is mainly due to two reasons. First, the frequencies associated with these Kaluza-Klein modes are smaller compared to general relativity (see Table VII as well as Fig. 8). Furthermore these Kaluza-Klein modes are supposed to be excited in the strong gravity regime, i.e., when mass of the black hole is large. On the other hand, as the mass of the black hole increases the frequency also decreases. This adds to the issue of detectability of these Kaluza-Klein modes. As evident from Table VII, for black hole mass $\sim 10^3 M_\odot$ the frequency of a mode in general relativity is within the limit of aLIGO detectors. However the same is not true for the Kaluza-Klein modes where the frequencies are smaller and hence possibly outside the operational band of the aLIGO detectors. Nonetheless, all these frequencies pertaining to higher mass black holes are very well within the operational domain of LISA and hence possibly detectable in near future (see Fig. 8). The second point corresponds to the Signal-to-Noise ratio, since in order to detect the signal it is necessary to generate oscillations having high Signal-to-Noise ratio. For this purpose as well we need collisions among heavier black holes (i.e., stronger gravity regime), so that higher order massive KK modes are excited. The frequency of these modes would correspondingly be lower and might get pushed out of the aLIGO frequency band but possibly be well within the LISA band.

While, the late time behaviour of these massive gravitational perturbation modes corresponds to a universal frequency, associated with the power-law tail of the wave mode and proportional to the Kaluza-Klein mode mass [68, 103]. Thus the frequency gets determined in terms of the d/ℓ ratio and the curvature length scale ℓ . Using the expression for n th Kaluza-Klein mode mass, $m_n = z_n(1/\ell) \exp(d/\ell)$, where z_n are the zeros of the Bessel function $J_{\sqrt{13}/2}(x)$ one immediately arrives at the desired expression for the late time frequency as a function of d/ℓ and $1/\ell$ respectively. Given this universal late time frequency, one immediately observes that as d/ℓ and $1/\ell$ increase, the frequency also increases and hence for a given d/ℓ ratio, the frequency will be in aLIGO band for a larger value of $1/\ell$, but will fall within the LISA band for smaller values of $1/\ell$ (as evident from Fig. 9 as well). This introduces additional complications in the detectability of these late time modes modulo the Gregory-Laflamme instability, which sets in for small $1/\ell$ values given a d/ℓ (see Fig. 9). At this point, it is interesting to note that given a black hole mass and a particular value of ℓ , the frequency bands of aLIGO and LISA set natural observational bounds on d/ℓ . In Fig. 9, we have considered two such scenarios, where the black hole masses are $50M_\odot$ and $10^5 M_\odot$, while $\ell = 1\mu\text{m}$. The scenarios are depicted by the thick green and blue lines respectively. As is clearly evident from the plot the modes from the $50M_\odot$ black hole can probe the range $17.0 < d/\ell < 23.9$. The $10^5 M_\odot$ black hole has only a limited probe for d/ℓ , because of the unstable configurations. The upper limit on d/ℓ in this case is therefore set by the boundary of the unstable region, so that $33.8 < d/\ell < 34.8$. Thus as long as the universal frequency spectrum is concerned, the late time behaviour of the Kaluza-Klein modes has a better chance of detection in aLIGO rather than in LISA as clearly

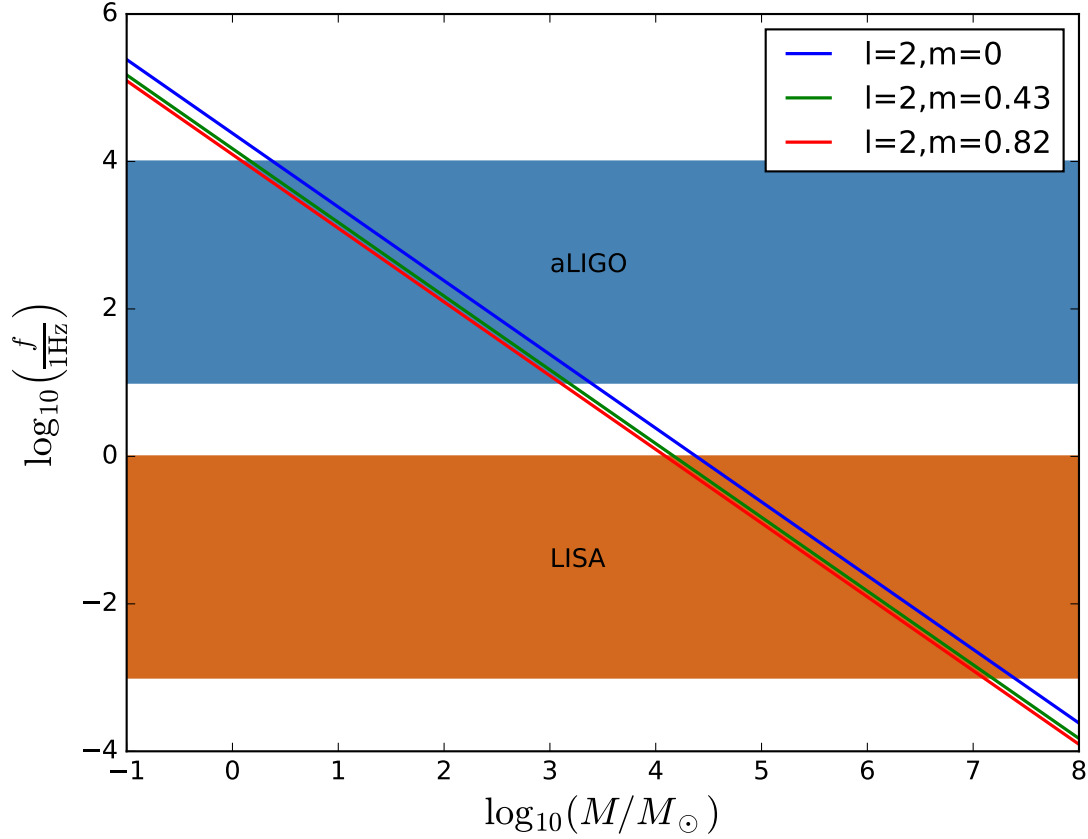


FIG. 8: The above figure depicts how the oscillation frequency of the gravitational wave in the ring down phase changes as the mass of the black hole increases. For convenience frequencies are plotted in Hz, while black hole mass has been presented in solar units, but both on a Logarithmic scale. The oscillation frequencies have been plotted in the brane based scenarios for two lowest lying Kaluza-Klein mode masses with $l = 2$. The same has been contrasted with the corresponding curve in general relativity. It is clear that for $M \sim 10^3 M_\odot$ the frequencies associated with general relativity are well within the aLIGO operational range, however for the massive Kaluza-Klein modes they are outside. Since these massive modes have better chance of getting detected in the high mass regime it is most likely that they may become observable once LISA is operational. See text for more discussions.

depicted in Fig. 9. The feasibility of the above detection, however is being determined by the Signal-to-Noise ratio, which will be much less for aLIGO while will be favourable for LISA. Hence even in this case there will be a tussle between the accessible regions in the $(d/\ell, 1/\ell)$ space and the Signal-to-Noise ratio making the detectability difficult for aLIGO detectors for the late time behaviour of the massive quasi-normal modes as well.

The above exercise also opens up a few future avenues to explore. We have discussed the effect of higher dimensions on the quasi-normal modes in this work, however it is possible to address the nature of quasi-bound states and in particular how the presence of extra dimensions affect them. This may provide another observational test bed for detection of higher spatial dimensions. Besides whether one can obtain similar results for the quasi-bound states from Cauchy evolution as well remains to be verified. Also a through analysis of this allowed region in light of the recent detection of gravitational waves in aLIGO can lead to possible constraints on the extra-dimensional parameter space. Moreover the effect of higher dimensions on neutron star equation of state parameter, tidal love numbers associated with a brane black hole can lead to exciting results which we are currently pursuing and will report elsewhere.

Acknowledgement

Research of S.C. is supported by the SERB-NPDF grant (PDF/2016/001589) from SERB, Government of India and the research of S.S.G is partially supported by the SERB-Extra Mural Research grant (EMR/2017/001372),

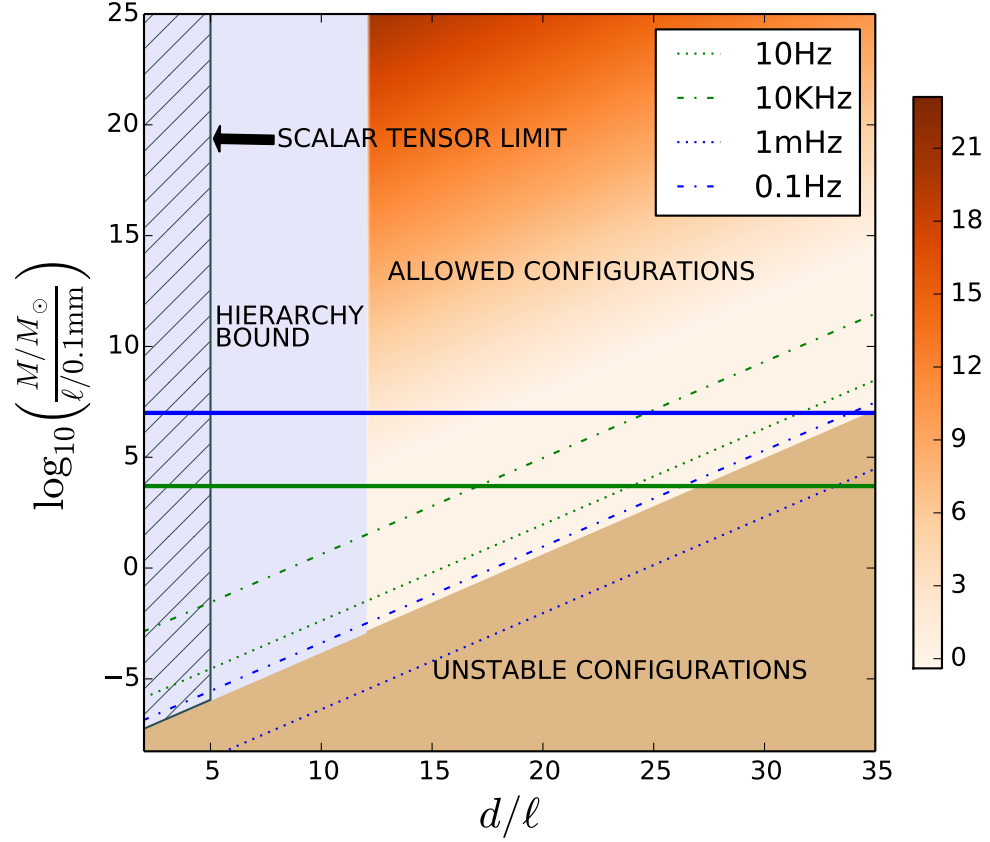


FIG. 9: The above figure depicts the allowed region in the $(d/\ell, M/\ell)$ plane along with the frequency associated with the very late time behaviour of the perturbation modes for black holes. The accessible region in the plot is obtained by imposing a few restrictions on the d/ℓ as well as M/ℓ values. These correspond to — (a) the Gregory-Laflamme instability, (b) the scalar-tensor limit and finally (c) the restriction on d/ℓ necessary to solve the hierarchy problem. The frequencies of the late time behaviour of the perturbation modes have been depicted in the accessible region by means of a colour coding. The labels on the right hand colour bar corresponds to a logarithm of frequencies (in Hz) to the base 10. The green dotted and dashed-dotted lines correspond to frequencies of 10 Hz and 10 KHz respectively, the extremities of aLIGO band. Similarly, the blue broken lines correspond to the extremities of the LISA band. The solid green and blue lines correspond to a configurations with $\ell\ell = 1\mu\text{m}$ and M being $50M_\odot$ and 10^5M_\odot respectively. For a given d/ℓ ratio as $1/\ell$ increases the frequency also increases, while for a given $1/\ell$, as d/ℓ increases the frequency decreases. Hence the aLIGO band is completely within the accessible region while the LISA band has substantial overlap with the unstable regions. See text for more discussions.

Government of India. This work was supported in part by NSF Grant PHY-1506497 and the Navajbai Ratan Tata Trust. The authors gratefully acknowledge discussions with David Hilditch, Emanuele Berti, Paolo Pani and Sanjeev Seahra. We also thank Shasvath Kapadia for carefully reading the manuscript and making useful suggestions. This work has been assigned the LIGO document number: LIGO-P1700295.

Appendix A: Deriving the perturbed gravitational field equations on the brane

In this appendix we present the detailed derivation of the perturbed gravitational field equations on the brane for completeness. We start with various geometrical quantities associated with spacetime curvature and express their

perturbative expansion to leading order in h_{AB} . These correspond to,

$$R_{ABCD}^{(h)} = \frac{1}{2} \left\{ \nabla_C \nabla_D h_{AB} + \nabla_C \nabla_B h_{AD} - \nabla_C \nabla_A h_{BD} \right. \\ \left. - \nabla_D \nabla_C h_{AB} - \nabla_D \nabla_B h_{AC} + \nabla_D \nabla_A h_{BC} \right\}, \quad (\text{A1})$$

$$R_{AB}^{(h)} = \frac{1}{2} \left\{ -\nabla_C \nabla^C h_{AB} - 2h_D^C R_{ACB}^{(g)} \right. \\ \left. + h_A^D R_{DB}^{(g)} + h_B^D R_{DA}^{(g)} \right\}, \quad (\text{A2})$$

$$R^{(h)} = \nabla_C \nabla_B h^{CB} - \nabla_C \nabla^C h = 0. \quad (\text{A3})$$

In order to arrive at the last line the gauge conditions introduced in Eq. (5) has been used. These gauge conditions further enables one to arrive at the following result,

$$\nabla_C \nabla_B h_A^C - \nabla_B \nabla_C h_A^C = h_A^D R_{DB}^{(g)} - h_D^C R_{ACB}^{(g)}, \quad (\text{A4})$$

which has also been used in deriving Eq. (A2). Since we are ultimately interested in perturbation equations on the brane, it is instructive to rewrite all the bulk quantities in terms of brane variables. In particular conversion of the bulk covariant derivatives to the brane covariant derivative is a necessary and important step in that direction, since these are the terms appearing in Eq. (A1), Eq. (A2) and Eq. (A3) respectively. This can be done by elaborating all the bulk covariant derivatives into ordinary derivatives and Christoffel connections and then picking up all the terms involving brane covariant derivatives as well as terms depending on the bulk curvature and derivative with respect to y . Further since $x^A = (y, x^\mu)$ it is clear that $e_\mu^A = \delta_\mu^A$. Thus we obtain from Eq. (A1),

$$2R_{ABCD}^{(h)} e_\mu^A n^B e_\nu^C n^D = 2\nabla_\nu \nabla_y h_{\mu y} - \nabla_\nu \nabla_\mu h_{yy} \\ - \nabla_y \nabla_\nu h_{\mu y} - \nabla_y \nabla_y h_{\mu\nu} + \nabla_y \nabla_\mu h_{y\nu} \\ = -\partial_y^2 h_{\mu\nu} - 2k\partial_y h_{\mu\nu}. \quad (\text{A5})$$

Two other contractions in Eq. (10) involving the perturbed Ricci tensor $R_{AB}^{(h)}$ results into,

$$R_{AC}^{(h)} e_\mu^A e_\nu^C = -\frac{1}{2} \nabla_C \nabla^C h_{\mu\nu} - h_\beta^\alpha R_{\mu\alpha\nu}^{(g)\beta} \\ + \frac{1}{2} h_\mu^\alpha R_{\alpha\nu}^{(g)} + \frac{1}{2} h_\nu^\alpha R_{\alpha\mu}^{(g)} \\ = -\frac{1}{2} {}^{(4)}\square h_{\mu\nu} - \frac{1}{2} \partial_y^2 h_{\mu\nu} + 3k^2 h_{\mu\nu} \\ - h_\beta^\alpha R_{\mu\alpha\nu}^{(g)\beta} + \frac{1}{2} h_\mu^\alpha R_{\alpha\nu}^{(g)} + \frac{1}{2} h_\nu^\alpha R_{\alpha\mu}^{(g)}, \quad (\text{A6})$$

and,

$$R_{AC}^{(h)} n^A n^C = -\frac{1}{2} \nabla_C \nabla^C h_{yy} - h_\beta^\alpha R_{y\alpha y}^{(g)\beta} = -h_\beta^\alpha R_{y\alpha y}^{(g)\beta}, \quad (\text{A7})$$

where Eq. (A2) has been used. In order to arrive at the previous expressions the gauge conditions presented in Eq. (5) have been used along with the following set of results,

$$g^{CD} \nabla_C \nabla_D h_{\alpha\beta} = {}^{(4)}\square h_{\alpha\beta} + \partial_y^2 h_{\alpha\beta} - 6k^2 h_{\alpha\beta} \\ \nabla_\nu \nabla_y h_{\mu y} = k\partial_y h_{\mu\nu} + 3k^2 h_{\mu\nu} \\ -\nabla_\nu \nabla_\mu h_{yy} = -2k^2 h_{\mu\nu} \\ -\nabla_y \nabla_\nu h_{y\mu} = -k\partial_y h_{\mu\nu} - 2k^2 h_{\mu\nu} \\ -\nabla_y \nabla_y h_{\mu\nu} = -\partial_y^2 h_{\mu\nu} - 4k\partial_y h_{\mu\nu} - 4k^2 h_{\mu\nu} \\ \nabla_y \nabla_\mu h_{y\nu} = k\partial_y h_{\mu\nu} + 2k^2 h_{\mu\nu}. \quad (\text{A8})$$

In arriving at the above relation we have also used the conditions that there exist only two non-vanishing connection components having the following forms: $\Gamma_{\mu\nu}^y = kq_{\mu\nu}$ and $\Gamma_{y\nu}^\mu = -k\delta_\nu^\mu$. Use of these expressions for various projections of Riemann and Ricci tensor from Eq. (A5), Eq. (A6) and Eq. (A7) in the perturbation equation for the bulk Weyl tensor as in Eq. (10) leads to,

$$\begin{aligned} E_{\mu\nu}^{(h)} = & \frac{1}{2} (-\partial_y^2 h_{\mu\nu} - 2k\partial_y h_{\mu\nu}) - \frac{1}{3} q_{\mu\nu} \left(-h_\beta^\alpha R_{y\alpha y}^{(g)\beta} \right) \\ & - \frac{1}{3} h_{\mu\nu} R_{yy}^{(g)} + \frac{1}{12} R^{(g)} h_{\mu\nu} \\ & - \frac{1}{3} \left(-\frac{1}{2} {}^{(4)}\square h_{\mu\nu} - \frac{1}{2} \partial_y^2 h_{\mu\nu} + 3k^2 h_{\mu\nu} \right. \\ & \left. - h^{\alpha\beta} R_{\mu\alpha\nu}^{(g)\beta} + \frac{1}{2} h_\mu^\alpha R_{\alpha\nu}^{(g)} + \frac{1}{2} h_\nu^\alpha R_{\alpha\mu}^{(g)} \right). \end{aligned} \quad (A9)$$

It is obvious that in order to separate out the perturbation of the bulk Weyl tensor into a four dimensional part and an additional part originating from extra dimensions, one needs to decompose all the quantities depending on the bulk metric g_{AB} in terms of the four dimensional metric $q_{\alpha\beta}$. For that purpose we consider the following decompositions,

$$\begin{aligned} R_{\mu\alpha\nu}^{(g)\beta} &= {}^{(4)}R_{\mu\alpha\nu}^{(q)\beta} - k^2 (q_{\mu\nu}\delta_\alpha^\beta - q_{\mu\alpha}\delta_\nu^\beta) \\ R_{y\alpha y}^{(g)\beta} &= -k^2 \delta_\alpha^\beta, \end{aligned} \quad (A10)$$

$$\begin{aligned} R_{\alpha\mu}^{(g)} &= {}^{(4)}R_{\alpha\mu}^{(q)} - 4k^2 q_{\alpha\mu} \\ R_{yy}^{(g)} &= -4k^2; \quad R^{(g)} = {}^{(4)}R^{(q)} - 20k^2. \end{aligned} \quad (A11)$$

This eventually results into Eq. (11).

Appendix B: Continued Fraction Method: Detailed Analysis

In this appendix, we provide a detailed and general derivation of the three term recursion relation pertaining to the continued fraction method, which we hope will be useful for the reader. Having derived Eq. (32) and Eq. (33) one normally makes an educated guess for $\psi_{n,l}$ and $\phi_{n,l}$ respectively. However as we will explicitly demonstrate this is not necessary. One can start with an arbitrary choice for $\psi_{n,l}$ and $\phi_{n,l}$, but the structure of the differential equation itself will lead to the correct expressions for the master variables. Following this philosophy we decompose $\psi_{n,l}$ and $\phi_{n,l}$ as follows,

$$\psi_{n,l} = (r-2)^\alpha r^\beta \exp(\lambda r) f_{n,l}(r), \quad (B1)$$

$$\phi_{n,l} = (r-2)^\alpha r^\beta \exp(\lambda r) g_{n,l}(r), \quad (B2)$$

where α , β and λ are arbitrary constants appearing in the master variables which we would like to uniquely determine using the structure of the differential equation. Substitution of these forms in Eq. (32) and Eq. (33) yields the following differential equations for $f_{n,l}$ and $g_{n,l}$ respectively,

$$\begin{aligned} r(r-2) \frac{d^2 f_{n,l}(r)}{dr^2} + \left\{ 2\lambda r^2 + (2\alpha + 2\beta - 4\lambda)r + (2 - 4\beta) \right\} \frac{df_{n,l}(r)}{dr} \\ + \left\{ (\lambda^2 - m_n^2) r^2 + (-2\lambda^2 + 2\alpha\lambda + 2\beta\lambda)r + \frac{\omega^2 r^3 + 2\alpha^2}{r-2} - \frac{2\beta^2 - 4\beta - 6}{r} \right. \\ \left. + (2\lambda - 4\beta\lambda + \beta(\beta-1) + \alpha(\alpha-1) - l(l+1) + 2\alpha\beta) \right\} f_{n,l}(r) - \frac{m_n^2}{r} g_{n,l} = 0, \end{aligned} \quad (B3)$$

$$\begin{aligned} r(r-2) \frac{d^2 g_{n,l}(r)}{dr^2} + \left\{ 2\lambda r^2 + (2\alpha + 2\beta - 4\lambda)r + (2 - 4\beta) \right\} \frac{dg_{n,l}(r)}{dr} \\ + \left\{ (\lambda^2 - m_n^2) r^2 + (-2\lambda^2 + 2\alpha\lambda + 2\beta\lambda)r + \frac{\omega^2 r^3 + 2\alpha^2}{r-2} - \frac{2\beta^2 - 4\beta}{r} \right. \\ \left. + (2\lambda - 4\beta\lambda + \beta(\beta-1) + \alpha(\alpha-1) - l(l+1) + 2\alpha\beta) \right\} f_{n,l}(r) - 4f_{n,l} = 0. \end{aligned} \quad (B4)$$

Given these differential equations one changes the variable from r to ξ , such that $r = 2/(1 - \xi)$. In order for these differential equations to have regular singular points after the variable change it is necessary that the terms behaving as r^2 , r and $1/(r - 2)$ in the above should vanish, which would require, at the first level, $\alpha = -2i\omega$. In which case one can use the following relation, $r^3 - 8 = (r - 2)(r^2 + 2r + 4)$, such that the other two parameters λ and β are determined as: $\lambda = \sqrt{m_n^2 - \omega^2}$, and $\beta = 2i\omega + (1/\lambda)(-\omega^2 + \lambda^2) = -(1/\lambda)(\omega - i\lambda)^2$. Hence the substitutions of these three constants leads to the following ansatz for the master variable suited with the above problem

$$\psi_{n,l} = \left(\frac{r-2}{r}\right)^{-2i\omega} r^{-b} e^{\lambda r} f_{n,l},$$

$$\lambda = \sqrt{m_n^2 - \omega^2}; \quad b = \frac{\omega^2 - \lambda^2}{\lambda}, \quad (B5)$$

$$\phi_{n,l} = \left(\frac{r-2}{r}\right)^{-2i\omega} r^{-b} e^{\lambda r} g_{n,l}. \quad (B6)$$

Using Eq. (B5) and Eq. (B6) respectively, both the differential equations can be casted in the following form,

$$r(r-2) \frac{d^2 y}{dr^2} + \left\{ Ar^2 + Br + C \right\} \frac{dy}{dr} + \left\{ D + \frac{E}{r} \right\} y + \left\{ F + \frac{G}{r} \right\} z = 0, \quad (B7)$$

where y stands for $f_{n,l}$ and z stands for $g_{n,l}$ or vice versa and the constants appearing in the above differential equation will depend on the parameters introduced above in Eq. (B5) and Eq. (B6). As mentioned earlier it is advantageous to introduce a new variable $\xi = (r - 2)/r$ in lieu of r , such that, $r = 2/(1 - \xi)$. Eliminating the variable r appearing in Eq. (B7) one can rewrite the differential equation in terms of the new variable ξ . Simplifying the resulting differential equation further we obtain,

$$\begin{aligned} \xi(1-\xi)^2 \frac{d^2 y}{d\xi^2} + \left\{ \left(2A + B + \frac{C}{2} \right) - (2 + B + C)\xi + \left(2 + \frac{C}{2} \right) \xi^2 \right\} \frac{dy}{d\xi} \\ + \left\{ \left(D + \frac{E}{2} \right) - \frac{E}{2}\xi \right\} y \\ + \left\{ \left(F + \frac{G}{2} \right) - \frac{G}{2}\xi \right\} z = 0. \end{aligned} \quad (B8)$$

The above differential equation can be solved using the power series technique. Keeping this in mind let us assume the following series expansion for y in powers of $(r - 2)/r$, or in terms of ξ as

$$y \equiv \sum_{j=0} c_j \left(\frac{r-2}{r} \right)^j = \sum_{j=0} c_j \xi^j; \quad z = \sum_{j=0} d_j \xi^j, \quad (B9)$$

where c_j and d_j are arbitrary coefficients that needs to be determined. Substitution of the above power series in the differential equation given by Eq. (B8) results into an equation involving various powers of ξ . Simplifying the above algebraic equation further and writing it in such a manner that all the powers of ξ coincides, we finally obtain the following three term recursion relation between three coefficients c_{j-1} , c_j and c_{j+1} as well as d_j and d_{j-1} appearing in the series expansion in Eq. (B9) as,

$$\begin{aligned} (j+1) \left(j + 2A + B + \frac{C}{2} \right) c_{j+1} - \left\{ 2j(j-1) + n(2 + B + C) - \left(D + \frac{E}{2} \right) \right\} c_j \\ + \left\{ (j-1)(j-2) + \left(2 + \frac{C}{2} \right) (j-1) - \frac{E}{2} \right\} c_{j-1} \\ + d_j \left(F + \frac{G}{2} \right) - \frac{G}{2} d_{j-1} = 0. \end{aligned} \quad (B10)$$

As we have mentioned earlier the same recursion relation holds for expansion coefficients of $f_{n,l}$ and $g_{n,l}$ both, but the constants appearing in the recursion relation will have distinct values for the two situations. In the case of $f_{n,l}$, we have, the following expressions for the constants,

$$\begin{aligned} A &= 2\lambda; & B &= 2\alpha + 2\beta - 4\lambda, \\ C &= 2 - 4\beta; & E &= -2\beta^2 + 4\beta + 6, \\ D &= 2\lambda - 4\beta\lambda + \beta(\beta - 1) + \alpha(\alpha - 1) \\ &\quad - l(l + 1) + 2\alpha\beta + 4\omega^2, \\ F &= 0; & G &= -m_n^2, \end{aligned} \tag{B11}$$

while, the corresponding values associated with the differential equation for $g_{n,l}$ becomes,

$$\begin{aligned} A &= 2\lambda; & B &= 2\alpha + 2\beta - 4\lambda, \\ C &= 2 - 4\beta; & E &= -2\beta^2 + 4\beta, \\ D &= 2\lambda - 4\beta\lambda + \beta(\beta - 1) + \alpha(\alpha - 1) \\ &\quad - l(l + 1) + 2\alpha\beta + 4\omega^2, \\ F &= -4; & G &= 0. \end{aligned} \tag{B12}$$

Using these constants one can write down the three term recursion relation for both the master variables, which we have used to arrive at Eq. (34).

-
- [1] A. Perez-Lorenzana, “An Introduction to extra dimensions,” *J. Phys. Conf. Ser.* **18** (2005) 224–269, [arXiv:hep-ph/0503177 \[hep-ph\]](#).
 - [2] C. Csaki, “TASI lectures on extra dimensions and branes,” in *From fields to strings: Circumnavigating theoretical physics. Ian Kogan memorial collection (3 volume set)*, pp. 605–698. 2004. [arXiv:hep-ph/0404096 \[hep-ph\]](#).
 - [3] R. Sundrum, “Tasi 2004 lectures: To the fifth dimension and back,” in *Theoretical Advanced Study Institute in Elementary Particle Physics: Many Dimensions of String Theory (TASI 2005) Boulder, Colorado, June 5–July 1, 2005*, pp. 585–630. 2005. [arXiv:hep-th/0508134 \[hep-th\]](#).
 - [4] J. Polchinski, *String theory. Vol. 1: An introduction to the bosonic string*. Cambridge University Press, 1998.
 - [5] J. Polchinski, *String theory. Vol. 2: Superstring theory and beyond*. Cambridge University Press, 1998.
 - [6] C. Rovelli, *Quantum gravity*. Cambridge University Press, 2004. <http://www.cambridge.org/uk/catalogue/catalogue.asp?isbn=0521837332>.
 - [7] S. Chakraborty, *Classical and Quantum Aspects of Gravity in Relation to The Emergent Paradigm*. Springer, 2017.
 - [8] N. Arkani-Hamed, S. Dimopoulos, and G. Dvali, “The Hierarchy problem and new dimensions at a millimeter,” *Phys.Lett.* **B429** (1998) 263–272, [arXiv:hep-ph/9803315 \[hep-ph\]](#).
 - [9] I. Antoniadis, N. Arkani-Hamed, S. Dimopoulos, and G. Dvali, “New dimensions at a millimeter to a Fermi and superstrings at a TeV,” *Phys.Lett.* **B436** (1998) 257–263, [arXiv:hep-ph/9804398 \[hep-ph\]](#).
 - [10] I. Antoniadis, “A Possible new dimension at a few TeV,” *Phys.Lett.* **B246** (1990) 377–384.
 - [11] V. Rubakov and M. Shaposhnikov, “Extra Space-Time Dimensions: Towards a Solution to the Cosmological Constant Problem,” *Phys.Lett.* **B125** (1983) 139.
 - [12] V. Rubakov and M. Shaposhnikov, “Do We Live Inside a Domain Wall?,” *Phys.Lett.* **B125** (1983) 136–138.
 - [13] L. Randall and R. Sundrum, “A Large mass hierarchy from a small extra dimension,” *Phys.Rev.Lett.* **83** (1999) 3370–3373, [arXiv:hep-ph/9905221 \[hep-ph\]](#).
 - [14] J. Garriga and T. Tanaka, “Gravity in the brane world,” *Phys.Rev.Lett.* **84** (2000) 2778–2781, [arXiv:hep-th/9911055 \[hep-th\]](#).
 - [15] A. Chamblin, S. Hawking, and H. Reall, “Brane world black holes,” *Phys.Rev.* **D61** (2000) 065007, [arXiv:hep-th/9909205 \[hep-th\]](#).
 - [16] E. Berti *et al.*, “Testing General Relativity with Present and Future Astrophysical Observations,” *Class. Quant. Grav.* **32** (2015) 243001, [arXiv:1501.07274 \[gr-qc\]](#).
 - [17] R. A. Konoplya and A. Zhidenko, “(In)stability of D-dimensional black holes in Gauss-Bonnet theory,” *Phys. Rev.* **D77** (2008) 104004, [arXiv:0802.0267 \[hep-th\]](#).
 - [18] R. A. Konoplya and A. Zhidenko, “Stability of multidimensional black holes: Complete numerical analysis,” *Nucl. Phys.* **B777** (2007) 182–202, [arXiv:hep-th/0703231 \[HEP-TH\]](#).
 - [19] E. Berti, V. Cardoso, and A. O. Starinets, “Quasinormal modes of black holes and black branes,” *Class. Quant. Grav.* **26** (2009) 163001, [arXiv:0905.2975 \[gr-qc\]](#).
 - [20] R. Gregory, “Braneworld black holes,” *Lect. Notes Phys.* **769** (2009) 259–298, [arXiv:0804.2595 \[hep-th\]](#).

- [21] R. Emparan, G. T. Horowitz, and R. C. Myers, “Exact description of black holes on branes,” *JHEP* **01** (2000) 007, [arXiv:hep-th/9911043 \[hep-th\]](#).
- [22] W. G. Cook, U. Sperhake, E. Berti, and V. Cardoso, “Black-hole head-on collisions in higher dimensions,” [arXiv:1709.10514 \[gr-qc\]](#).
- [23] C. Csaki, M. Graesser, L. Randall, and J. Terning, “Cosmology of brane models with radion stabilization,” *Phys.Rev.* **D62** (2000) 045015, [arXiv:hep-ph/9911406 \[hep-ph\]](#).
- [24] C. Csaki, M. Graesser, C. F. Kolda, and J. Terning, “Cosmology of one extra dimension with localized gravity,” *Phys.Lett.* **B462** (1999) 34–40, [arXiv:hep-ph/9906513 \[hep-ph\]](#).
- [25] P. Binetruy, C. Deffayet, and D. Langlois, “Nonconventional cosmology from a brane universe,” *Nucl.Phys.* **B565** (2000) 269–287, [arXiv:hep-th/9905012 \[hep-th\]](#).
- [26] D. Ida, “Brane world cosmology,” *JHEP* **0009** (2000) 014, [arXiv:gr-qc/9912002 \[gr-qc\]](#).
- [27] S. Nojiri, S. D. Odintsov, and S. Ogushi, “Cosmological and black hole brane world universes in higher derivative gravity,” *Phys. Rev.* **D65** (2002) 023521, [arXiv:hep-th/0108172 \[hep-th\]](#).
- [28] S. Nojiri, S. D. Odintsov, and S. Ogushi, “Friedmann-Robertson-Walker brane cosmological equations from the five-dimensional bulk (A)dS black hole,” *Int. J. Mod. Phys.* **A17** (2002) 4809–4870, [arXiv:hep-th/0205187 \[hep-th\]](#).
- [29] C. Charmousis and J.-F. Dufaux, “General Gauss-Bonnet brane cosmology,” *Class. Quant. Grav.* **19** (2002) 4671–4682, [arXiv:hep-th/0202107 \[hep-th\]](#).
- [30] C. Germani and C. F. Sopuerta, “String inspired brane world cosmology,” *Phys. Rev. Lett.* **88** (2002) 231101, [arXiv:hep-th/0202060 \[hep-th\]](#).
- [31] E. Gravanis and S. Willison, “Israel conditions for the Gauss-Bonnet theory and the Friedmann equation on the brane universe,” *Phys. Lett.* **B562** (2003) 118–126, [arXiv:hep-th/0209076 \[hep-th\]](#).
- [32] P. Brax, C. van de Bruck, and A.-C. Davis, “Brane world cosmology,” *Rept.Prog.Phys.* **67** (2004) 2183–2232, [arXiv:hep-th/0404011 \[hep-th\]](#).
- [33] W. D. Goldberger and M. B. Wise, “Phenomenology of a stabilized modulus,” *Phys. Lett.* **B475** (2000) 275–279, [arXiv:hep-ph/9911457 \[hep-ph\]](#).
- [34] H. Davoudiasl, J. Hewett, and T. Rizzo, “Bulk gauge fields in the Randall-Sundrum model,” *Phys.Lett.* **B473** (2000) 43–49, [arXiv:hep-ph/9911262 \[hep-ph\]](#).
- [35] H. Davoudiasl, J. Hewett, and T. Rizzo, “Experimental probes of localized gravity: On and off the wall,” *Phys.Rev.* **D63** (2001) 075004, [arXiv:hep-ph/0006041 \[hep-ph\]](#).
- [36] W. D. Goldberger and M. B. Wise, “Modulus stabilization with bulk fields,” *Phys.Rev.Lett.* **83** (1999) 4922–4925, [arXiv:hep-ph/9907447 \[hep-ph\]](#).
- [37] Z. Chacko and A. E. Nelson, “A Solution to the hierarchy problem with an infinitely large extra dimension and moduli stabilization,” *Phys.Rev.* **D62** (2000) 085006, [arXiv:hep-th/9912186 \[hep-th\]](#).
- [38] S. Chakraborty and S. SenGupta, “Higher curvature gravity at the LHC,” *Phys.Rev.* **D90** no. 4, (2014) 047901, [arXiv:1403.3164 \[gr-qc\]](#).
- [39] S. Chakraborty and S. Sengupta, “Radion cosmology and stabilization,” *Eur.Phys.J.* **C74** no. 9, (2014) 3045, [arXiv:1306.0805 \[gr-qc\]](#).
- [40] S. Chakraborty and S. SenGupta, “Gravity stabilizes itself,” *Eur. Phys. J.* **C77** (2017) 573, [arXiv:1701.01032 \[gr-qc\]](#).
- [41] I. Banerjee, S. Chakraborty, and S. SenGupta, “Excavating black hole continuum spectrum: Possible signatures of scalar hairs and of higher dimensions,” [arXiv:1707.04494 \[gr-qc\]](#).
- [42] S. Chakraborty and S. SenGupta, “Strong gravitational lensing — A probe for extra dimensions and Kalb-Ramond field,” *JCAP* **1707** no. 07, (2017) 045, [arXiv:1611.06936 \[gr-qc\]](#).
- [43] **VIRGO, LIGO Scientific** Collaboration, B. P. Abbott *et al.*, “GW170104: Observation of a 50-Solar-Mass Binary Black Hole Coalescence at Redshift 0.2,” *Phys. Rev. Lett.* **118** no. 22, (2017) 221101, [arXiv:1706.01812 \[gr-qc\]](#).
- [44] **Virgo, LIGO Scientific** Collaboration, B. P. Abbott *et al.*, “Binary Black Hole Mergers in the first Advanced LIGO Observing Run,” *Phys. Rev.* **X6** no. 4, (2016) 041015, [arXiv:1606.04856 \[gr-qc\]](#).
- [45] **Virgo, LIGO Scientific** Collaboration, B. P. Abbott *et al.*, “GW151226: Observation of Gravitational Waves from a 22-Solar-Mass Binary Black Hole Coalescence,” *Phys. Rev. Lett.* **116** no. 24, (2016) 241103, [arXiv:1606.04855 \[gr-qc\]](#).
- [46] **Virgo, LIGO Scientific** Collaboration, B. P. Abbott *et al.*, “Tests of general relativity with GW150914,” *Phys. Rev. Lett.* **116** no. 22, (2016) 221101, [arXiv:1602.03841 \[gr-qc\]](#).
- [47] **Virgo, LIGO Scientific** Collaboration, B. P. Abbott *et al.*, “Observation of Gravitational Waves from a Binary Black Hole Merger,” *Phys. Rev. Lett.* **116** no. 6, (2016) 061102, [arXiv:1602.03837 \[gr-qc\]](#).
- [48] H. Asada, M. Shibata, and T. Futamase, “PostNewtonian hydrodynamic equations using the (3+1) formalism in general relativity,” *Prog. Theor. Phys.* **96** (1996) 81–112, [arXiv:gr-qc/9606041 \[gr-qc\]](#).
- [49] T. Damour, P. Jaranowski, and G. Schaefer, “Effective one body approach to the dynamics of two spinning black holes with next-to-leading order spin-orbit coupling,” *Phys. Rev.* **D78** (2008) 024009, [arXiv:0803.0915 \[gr-qc\]](#).
- [50] T. Damour, “Coalescence of two spinning black holes: an effective one-body approach,” *Phys. Rev.* **D64** (2001) 124013, [arXiv:gr-qc/0103018 \[gr-qc\]](#).
- [51] A. Nagar, “Effective one body Hamiltonian of two spinning black-holes with next-to-next-to-leading order spin-orbit coupling,” *Phys. Rev.* **D84** (2011) 084028, [arXiv:1106.4349 \[gr-qc\]](#). [Erratum: *Phys. Rev.* **D88**, no. 8, 089901 (2013)].
- [52] T. Damour, B. R. Iyer, and A. Nagar, “Improved resummation of post-Newtonian multipolar waveforms from circularized compact binaries,” *Phys. Rev.* **D79** (2009) 064004, [arXiv:0811.2069 \[gr-qc\]](#).
- [53] L. Baiotti, T. Damour, B. Giacomazzo, A. Nagar, and L. Rezzolla, “Analytic modelling of tidal effects in the relativistic inspiral of binary neutron stars,” *Phys. Rev. Lett.* **105** (2010) 261101, [arXiv:1009.0521 \[gr-qc\]](#).

- [54] L. Blanchet, “Gravitational radiation from post-Newtonian sources and inspiralling compact binaries,” *Living Rev. Rel.* **9** (2006) 4.
- [55] E. E. Flanagan and S. A. Hughes, “The Basics of gravitational wave theory,” *New J. Phys.* **7** (2005) 204, [arXiv:gr-qc/0501041 \[gr-qc\]](#).
- [56] J. Centrella, J. G. Baker, B. J. Kelly, and J. R. van Meter, “Black-hole binaries, gravitational waves, and numerical relativity,” *Rev. Mod. Phys.* **82** (2010) 3069, [arXiv:1010.5260 \[gr-qc\]](#).
- [57] P. Ajith *et al.*, “A Template bank for gravitational waveforms from coalescing binary black holes. I. Non-spinning binaries,” *Phys. Rev.* **D77** (2008) 104017, [arXiv:0710.2335 \[gr-qc\]](#). [Erratum: *Phys. Rev.* **D79**, 129901(2009)].
- [58] A. Buonanno and T. Damour, “Transition from inspiral to plunge in binary black hole coalescences,” *Phys. Rev.* **D62** (2000) 064015, [arXiv:gr-qc/0001013 \[gr-qc\]](#).
- [59] T. Delsate, D. Hilditch, and H. Witek, “Initial value formulation of dynamical Chern-Simons gravity,” *Phys. Rev.* **D91** no. 2, (2015) 024027, [arXiv:1407.6727 \[gr-qc\]](#).
- [60] A. Pai, S. Dhurandhar, and S. Bose, “A Data analysis strategy for detecting gravitational wave signals from inspiraling compact binaries with a network of laser interferometric detectors,” *Phys. Rev.* **D64** (2001) 042004, [arXiv:gr-qc/0009078 \[gr-qc\]](#).
- [61] S. Bose, “Search templates for stochastic gravitational-wave backgrounds,” *Phys. Rev.* **D71** (2005) 082001, [arXiv:astro-ph/0504048 \[astro-ph\]](#).
- [62] F. Pretorius, “Evolution of binary black hole spacetimes,” *Phys. Rev. Lett.* **95** (2005) 121101, [arXiv:gr-qc/0507014 \[gr-qc\]](#).
- [63] K. G. Arun, B. R. Iyer, M. S. S. Qusailah, and B. S. Sathyaprakash, “Testing post-Newtonian theory with gravitational wave observations,” *Class. Quant. Grav.* **23** (2006) L37–L43, [arXiv:gr-qc/0604018 \[gr-qc\]](#).
- [64] P. Kanti and R. A. Konoplya, “Quasi-normal modes of brane-localised standard model fields,” *Phys. Rev.* **D73** (2006) 044002, [arXiv:hep-th/0512257 \[hep-th\]](#).
- [65] R. A. Konoplya and A. Zhidenko, “Quasinormal modes of black holes: From astrophysics to string theory,” *Rev. Mod. Phys.* **83** (2011) 793–836, [arXiv:1102.4014 \[gr-qc\]](#).
- [66] B. Toshmatov, Z. Stuchlik, J. Schee, and B. Ahmedov, “Quasinormal frequencies of black hole in the braneworld,” *Phys. Rev.* **D93** no. 12, (2016) 124017, [arXiv:1605.02058 \[gr-qc\]](#).
- [67] D. Andriot and G. Lucena Gmez, “Signatures of extra dimensions in gravitational waves,” *JCAP* **1706** no. 06, (2017) 048, [arXiv:1704.07392 \[hep-th\]](#).
- [68] S. S. Seahra, C. Clarkson, and R. Maartens, “Detecting extra dimensions with gravity wave spectroscopy: the black string brane-world,” *Phys. Rev. Lett.* **94** (2005) 121302, [arXiv:gr-qc/0408032 \[gr-qc\]](#).
- [69] C. Clarkson and R. Maartens, “Gravity-wave detectors as probes of extra dimensions,” *Gen. Rel. Grav.* **37** (2005) 1681–1687, [arXiv:astro-ph/0505277 \[astro-ph\]](#). [*Int. J. Mod. Phys.* **D14**, 2347(2005)].
- [70] S. S. Seahra and C. Clarkson, “Gravitational waves in the black string braneworld,” *Class. Quant. Grav.* **26** (2009) 245004, [arXiv:0907.2174 \[gr-qc\]](#).
- [71] C. Clarkson and S. S. Seahra, “A gravitational wave window on extra dimensions,” *Class. Quant. Grav.* **24** (2007) F33–F40, [arXiv:astro-ph/0610470 \[astro-ph\]](#).
- [72] C. Clarkson and S. S. Seahra, “Braneworld resonances,” *Class. Quant. Grav.* **22** (2005) 3653–3688, [arXiv:gr-qc/0505145 \[gr-qc\]](#).
- [73] S. S. Seahra, “Gravitational waves from braneworld black holes,” *Lect. Notes Phys.* **769** (2009) 347–386.
- [74] H. Witek, “Numerical Relativity in higher-dimensional space-times,” *Int. J. Mod. Phys.* **A28** (2013) 1340017, [arXiv:1308.1686 \[gr-qc\]](#).
- [75] T. Shiromizu, K.-i. Maeda, and M. Sasaki, “The Einstein equation on the 3-brane world,” *Phys. Rev.* **D62** (2000) 024012, [arXiv:gr-qc/9910076 \[gr-qc\]](#).
- [76] S. Chakraborty and S. SenGupta, “Spherically symmetric brane spacetime with bulk $f(\mathcal{R})$ gravity,” *Eur. Phys. J.* **C75** no. 1, (2015) 11, [arXiv:1409.4115 \[gr-qc\]](#).
- [77] S. Chakraborty and S. SenGupta, “Effective gravitational field equations on m -brane embedded in n -dimensional bulk of Einstein and $f(\mathcal{R})$ gravity,” *Eur. Phys. J.* **C75** no. 11, (2015) 538, [arXiv:1504.07519 \[gr-qc\]](#).
- [78] S. Chakraborty and S. SenGupta, “Spherically symmetric brane in a bulk of $f(R)$ and Gauss-Bonnet Gravity,” *Class. Quant. Grav.* **33** no. 22, (2016) 225001, [arXiv:1510.01953 \[gr-qc\]](#).
- [79] T. Padmanabhan, *Gravitation: Foundations and Frontiers*. Cambridge University Press, Cambridge, UK, 2010.
- [80] E. Poisson, *A Relativist’s Toolkit: The Mathematics of Black-Hole Mechanics*. Cambridge University Press, 1st ed., 2007.
- [81] R. Maartens, “Geometry and dynamics of the brane world,” in *Spanish Relativity Meeting on Reference Frames and Gravitomagnetism (ERES2000) Valladolid, Spain, September 6-9, 2000*. 2001. [arXiv:gr-qc/0101059 \[gr-qc\]](#). <http://alice.cern.ch/format/showfull?sysnb=2237527>.
- [82] N. Dadhich, R. Maartens, P. Papadopoulos, and V. Rezanian, “Black holes on the brane,” *Phys. Lett.* **B487** (2000) 1–6, [arXiv:hep-th/0003061 \[hep-th\]](#).
- [83] T. Harko and M. Mak, “Vacuum solutions of the gravitational field equations in the brane world model,” *Phys. Rev.* **D69** (2004) 064020, [arXiv:gr-qc/0401049 \[gr-qc\]](#).
- [84] R. Maartens and K. Koyama, “Brane-World Gravity,” *Living Rev. Rel.* **13** (2010) 5, [arXiv:1004.3962 \[hep-th\]](#).
- [85] S. Bhattacharyya and S. Shankaranarayanan, “Quasinormal modes as a distinguisher between general relativity and $f(R)$ gravity,” *Phys. Rev.* **D96** no. 6, (2017) 064044, [arXiv:1704.07044 \[gr-qc\]](#).
- [86] G. Pratten, “Covariant Perturbations of $f(R)$ Black Holes: The Weyl Terms,” *Class. Quant. Grav.* **32** no. 16, (2015) 165018, [arXiv:1503.03435 \[gr-qc\]](#).

- [87] A. Chamblin, H. S. Reall, H.-a. Shinkai, and T. Shiromizu, “Charged brane world black holes,” *Phys. Rev.* **D63** (2001) 064015, [arXiv:hep-th/0008177 \[hep-th\]](#).
- [88] N. Dadhich and S. G. Ghosh, “Gravitational collapse of null fluid on the brane,” *Phys. Lett.* **B518** (2001) 1–7, [arXiv:hep-th/0101019 \[hep-th\]](#).
- [89] C. D. Hoyle, D. J. Kapner, B. R. Heckel, E. G. Adelberger, J. H. Gundlach, U. Schmidt, and H. E. Swanson, “Sub-millimeter tests of the gravitational inverse-square law,” *Phys. Rev.* **D70** (2004) 042004, [arXiv:hep-ph/0405262 \[hep-ph\]](#).
- [90] J. C. Long, H. W. Chan, A. B. Churnside, E. A. Gulbis, M. C. M. Varney, and J. C. Price, “Upper limits to submillimeter-range forces from extra space-time dimensions,” [arXiv:hep-ph/0210004 \[hep-ph\]](#). [Nature421,922(2003)].
- [91] S. J. Smullin, A. A. Geraci, D. M. Weld, J. Chilverini, S. P. Holmes, and A. Kapitulnik, “New constraints on Yukawa-type deviations from Newtonian gravity at 20 microns,” *Phys. Rev.* **D72** (2005) 122001, [arXiv:hep-ph/0508204 \[hep-ph\]](#). [Erratum: Phys. Rev.D72,129901(2005)].
- [92] R. Gregory, “Black string instabilities in Anti-de Sitter space,” *Class. Quant. Grav.* **17** (2000) L125–L132, [arXiv:hep-th/0004101 \[hep-th\]](#).
- [93] R. Gregory, “The Gregory-Laflamme instability,” in *Black holes in higher dimensions*, G. T. Horowitz, ed., pp. 29–43. 2011. [arXiv:1107.5821 \[gr-qc\]](#). <https://inspirehep.net/record/921476/files/arXiv:1107.5821.pdf>.
- [94] L. Lehner and F. Pretorius, “Final State of Gregory-Laflamme Instability,” [arXiv:1106.5184 \[gr-qc\]](#).
- [95] V. P. Frolov and A. A. Shoom, “Gregory-Laflamme instability of 5D electrically charged black strings,” *Phys. Rev.* **D79** (2009) 104002, [arXiv:0903.2893 \[hep-th\]](#).
- [96] R. A. Konoplya, K. Murata, J. Soda, and A. Zhidenko, “Looking at the Gregory-Laflamme instability through quasi-normal modes,” *Phys. Rev.* **D78** (2008) 084012, [arXiv:0807.1897 \[hep-th\]](#).
- [97] E. W. Leaver, “An Analytic representation for the quasi normal modes of Kerr black holes,” *Proc. Roy. Soc. Lond.* **A402** (1985) 285–298.
- [98] S. Chandrasekhar, “The mathematical theory of black holes,” in *Oxford, UK: Clarendon (1992) 646 p., OXFORD, UK: CLARENDON (1985) 646 P.* 1985.
- [99] H.-P. Nollert, “TOPICAL REVIEW: Quasinormal modes: the characteristic ‘sound’ of black holes and neutron stars,” *Class. Quant. Grav.* **16** (1999) R159–R216.
- [100] K. D. Kokkotas and B. G. Schmidt, “Quasinormal modes of stars and black holes,” *Living Rev. Rel.* **2** (1999) 2, [arXiv:gr-qc/9909058 \[gr-qc\]](#).
- [101] P. Pani, “Advanced Methods in Black-Hole Perturbation Theory,” *Int. J. Mod. Phys.* **A28** (2013) 1340018, [arXiv:1305.6759 \[gr-qc\]](#).
- [102] V. Cardoso, S. Chakrabarti, P. Pani, E. Berti, and L. Gualtieri, “Floating and sinking: The Imprint of massive scalars around rotating black holes,” *Phys. Rev. Lett.* **107** (2011) 241101, [arXiv:1109.6021 \[gr-qc\]](#).
- [103] J. G. Rosa and S. R. Dolan, “Massive vector fields on the Schwarzschild spacetime: quasi-normal modes and bound states,” *Phys. Rev.* **D85** (2012) 044043, [arXiv:1110.4494 \[hep-th\]](#).
- [104] R. A. Konoplya and A. Zhidenko, “Stability of higher dimensional Reissner-Nordstrom-anti-de Sitter black holes,” *Phys. Rev.* **D78** (2008) 104017, [arXiv:0809.2048 \[hep-th\]](#).
- [105] R. A. Konoplya and A. Zhidenko, “Stability and quasinormal modes of the massive scalar field around Kerr black holes,” *Phys. Rev.* **D73** (2006) 124040, [arXiv:gr-qc/0605013 \[gr-qc\]](#).